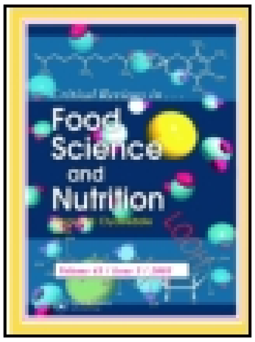

Critical Reviews in Food Science and Nutrition

ISSN: (Print) (Online) Journal homepage: https://www.tandfonline.com/loi/bfsn20

Thermo-mechanical processing of plant proteins using shear cell and high-moisture extrusion cooking

Steven H. V. Cornet , Silvia J. E. Snel , Floor K. G. Schreuders , Ruud G. M. van der Sman , Michael Beyrer & Atze Jan van der Goot

To cite this article: Steven H. V. Cornet , Silvia J. E. Snel , Floor K. G. Schreuders , Ruud G. M. van der Sman , Michael Beyrer & Atze Jan van der Goot (2021): Thermo-mechanical processing of plant proteins using shear cell and high-moisture extrusion cooking, Critical Reviews in Food Science and Nutrition, DOI: 10.1080/10408398.2020.1864618

To link to this article: https://doi.org/10.1080/10408398.2020.1864618

CRITICAL REVIEWS IN FOOD SCIENCE AND NUTRITION
https://doi.org/10.1080/10408398.2020.1864618

Taylor & Francis
Taylor & Francis Group

REVIEW

Thermo-mechanical processing of plant proteins using shear cell and high-moisture extrusion cooking

Steven H. V. Cornet[a,b$], Silvia J. E. Snel[a,c#$], Floor K. G. Schreuders[a], Ruud G. M. van der Sman[a,b], Michael Beyrer[c#], and Atze Jan van der Goot[a]

[a]Food Process Engineering, Agrotechnology and Food Sciences Group, Wageningen University & Research, Wageningen, The Netherlands; [b]Food and Biobased Research, Wageningen University & Research, Wageningen, The Netherlands; [c]Food Process Engineering, School of Engineering, Sion, The Netherlands

ABSTRACT
Consumption of plant-based meat analogues offers a way to reduce the environmental footprint of the human diet. High-moisture extrusion cooking (HMEC) and shear cell processing both rely on thermo-mechanical treatment of proteins to product fibrous meat-like products. However, the mechanisms underlying these processes are not well understood. In this review we discuss the effect of thermo-mechanical processing on the physicochemical properties and phase behavior of proteins and protein mixtures. The HMEC and shear cell processes are comparable in their basic unit operations, which are (1) mixing and hydration, (2) thermo-mechanical treatment, and (3) cooling. An often overlooked part of the extruder that could be crucial to fibrillation is the so-called breaker plate, which is situated between the barrel and die sections. We found a lack of consensus on the effect of heat on protein-protein interactions, and that the experimental tools to study protein-protein interactions are limited. The different mechanisms for structure formation proposed in literature all consider the deformation and alignment of the melt. However, the mechanisms differ in their underlying assumptions. Further investigation using novel and dedicated tools is required to fully understand these thermo-mechanical processes.

KEYWORDS
Meat analogue; phase deformation; plant proteins; polymer melt; structuring mechanisms

Introduction

Reducing the amount of animal protein in our diet is considered essential to improving the sustainability of our diet (Aiking and de Boer 2020; Chaudhary, Gustafson, and Mathys 2018; Pimentel and Pimentel 2003). One strategy toward achieving this protein transition is to offer consumers a plant-based alternative to meat. Meat-eating consumers would prefer products that strongly resemble real meat (Hoek 2010). This is stimulating the development of plant-based meat analogues and the technologies used to produce them. Technologies capable of producing a fibrous, meat-like structure from plant-based ingredients are electro-spinning (Nieuwland et al. 2014), high-moisture extrusion cooking (HMEC) (Chiang et al. 2019), and shear cell technology (Grabowska et al. 2014; Krintiras et al. 2016). Of these three technologies, only extrusion cooking is currently used industrially for the production of meat analogues. Electro-spinning of food-grade protein fibers has recently seen several developments (Nieuwland et al. 2014; Kutzli et al. 2019; Leidy and Maria Ximena 2019; Mendes, Stephansen, and Chronakis 2017). However, the electro-spinning of proteins is considered notoriously difficult, uses large amounts of water or organic solvents, and upscaling poses a challenge (Nieuwland et al. 2014; Manski, van der Goot, and Boom 2007a). Shear cell devices were initially developed to study the extrusion process (Einde, Goot, and Boom 2003; Peighambardoust et al. 2004), and were later identified as a novel structuring technique (Manski, van der Goot, and Boom 2007b; Grabowska et al. 2014). The shear cell and HMEC processes both rely on thermo-mechanical stresses to create fibrous structures and are the focus of this review.

The thermo-mechanical processing of proteins is often studied for non-food products such as bio-plastics (Klüver and Meyer 2015; Ralston and Osswald 2008), and food products such as meat analogues (Samard, Gu, and Ryu 2019). Several recent studies have explored the effect of process parameters such as specific mechanical energy (SME) (Fang, Zhang, and Wei 2014; Pietsch, Emin, and Schuchmann 2017), shear rate (Dekkers, Hamoen, et al. 2018), and temperature (Pietsch, Emin, and Schuchmann 2017; Schreuders et al. 2019; Dekkers, Nikiforidis, et al. 2016) on food product properties. Still, formulation development and ingredient screening

---

CONTACT Atze Jan van der Goot atzejan.vandergoot@wur.nl Food Process Engineering, Agrotechnology and Food Sciences Group, Wageningen University & Research, Bornse Weilanden 9, 6708 WG Wageningen, The Netherlands.

[$] These authors contributed equally

[#] Present address: Institute of Life Technologies, University of Applied Sciences and Arts Western Switzerland, Sion, Switzerland.

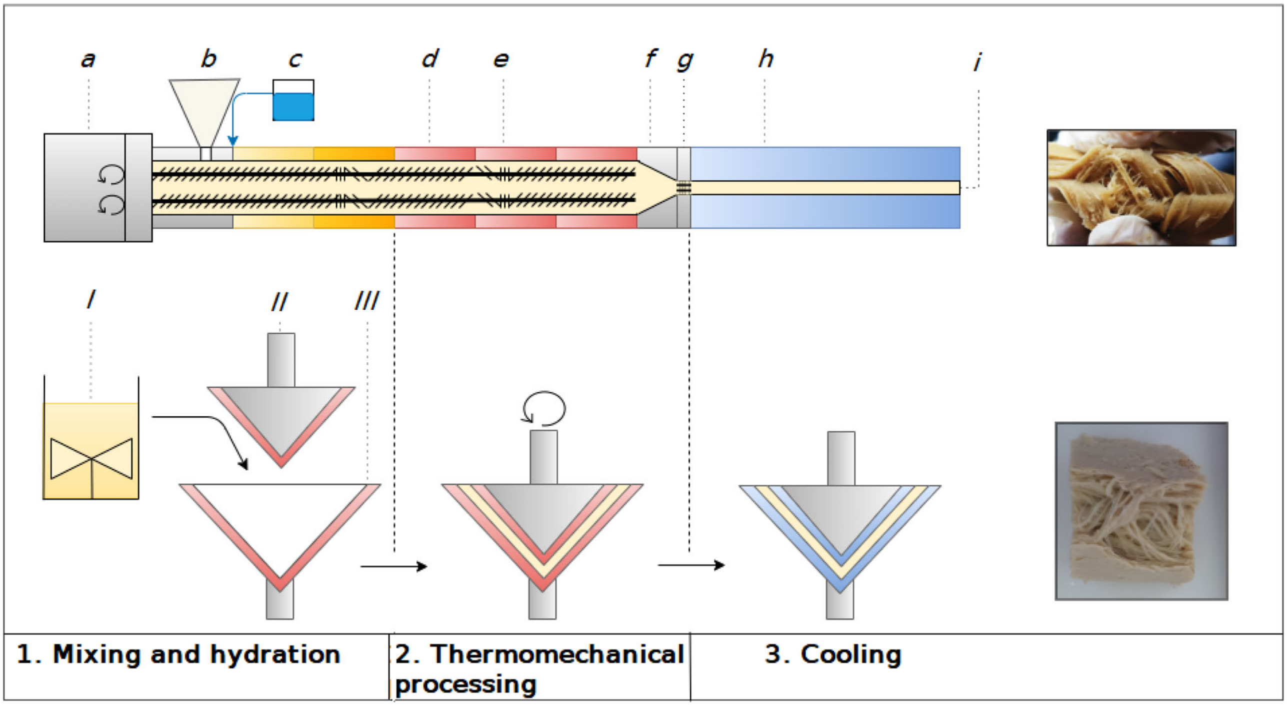

Figure 1. Schematic representation of an extruder and a conical shear cell. The different sections of the extruder are indicated with letters: *a*, motor; *b*, (dry) feeder; *c*, water pump; *d*, extruder barrel with screws; *e*, kneading blocks; *f*, transition zone; *g*, breaker plate; *h*, cooling die; *i*, die outlet. The different sections of the shear cell are indicated with roman numbers: *I*, external mixer for dry and wet ingredients; *II*, stationary top cone; *III*, rotating bottom cone. Extrudate picture was reproduced from Samard, Gu, and Ryu (2019) with permission.

lean heavily on empirical knowledge and trial-and-error based experimentation. Greater insight into the effect of the different processing steps would streamline product development and could lead to improved ingredient flexibility and process stability.

Although extrusion processes have been studied for several decades, the field is still at an exploratory stage. This paper provides a review of the thermo-mechanical structuring of plant-based proteins. Both the shear cell and HMEC processes will be considered. The paper is organized as follows. First the unit operations of the shear cell and HMEC processes are described. Then we go through the different unit operations step-by-step and discuss the physicochemical and phase changes that are induced by the process. The different mechanisms for structure formation posed in the literature will be discussed, and we will reflect on some of the predominant experimental approaches described in the literature. We will conclude with a general discussion in which we identify the current knowledge gaps and provide an outlook for future research.

Process description

The HMEC and shear cell processes both make use of thermo-mechanical treatment to create fibrous structures. The processes are comparable in their basic unit operations and comprise of a mixing and hydration step, thermo-mechanical treatment, and a cooling step (Figure 1). Furthermore, the formulations that have led to a fibrous structure are similar between the two technologies (Table 1). Both use leguminous protein isolates or concentrates from e.g. soy, fababean or pea, often in combination with gluten or a polysaccharide (Table 1). Other less conventional protein sources have also led to favorable outcomes, such as peanut protein, microalgae, or non-refined soy flour (Table 1). Water contents used in HMEC and shear cell processing are comparable and range from approximately 50 to 70%.

High-moisture extrusion cooking

The application of extrusion cooking for the production of meat-like products started in the 1970s using primarily soy (Puski and Konwinski 1976). These meat-like products were expanded and had to be hydrated before use (Campbell 1981). Expansion of the extrudate can occur due to the pressure drop upon exiting the die. This can lead to boiling and the rapid evaporation of water and results in a spongy texture (Samard, Gu, and Ryu 2019). The use of a long cooling die can be used to prevent the product from expanding and has enabled the extrusion of materials with a high moisture content (Cheftel, Kitagawa, and Queguiner 1992). HMEC can be defined as extrusion with a cooling die and a water content exceeding 50% (Caporgno et al. 2020), which is also reflected by the compositions listed in Table 1.

An extruder consists of a heated barrel (Figure 1*d*) equipped with one or two screws driven by a motor (Figure 1*a*), a transition zone (Figure 1*f*), and a cooling die (Figure 1*h*). Twin-screw extruders with co-rotating screws are mostly used for the production of meat analogues, although some have also used single screw extruders (Table 1). Dry and wet ingredients are fed separately into the extruder barrel at the desired feed rates (Figure 1*b*, *c*). The extruder barrel consists of different sections that can be heated individually. The co-rotating motion of the screws provides

Table 1. An overview of plant-based ingredients and combinations thereof, and process conditions used to produce fibrous structures through thermo-mechanical processing.

Technique	Material	Moisture content (%)	Maximum temperature (°C)	References
TSE	SPC + MA	60	140	Caporgno et al. (2020)
SC	PPI + WG	60	95–140	Schreuders et al. (2020)
TSE	PP	55	155	Zhang et al. (2020)
SC	FPI + WG	61.5	140	Cornet et al. (2020)
TSE	SPC + WG	60	170	Chiang et al. (2019)
TSE	LPI + MA	50	140–175	Palanisamy et al. (2019)
TSE	SPC	60	100, 140, 160	Pietsch et al. (2019)
TSE	SPI + WG + CS	70	160	Samard, Gu, and Ryu (2019)
SC	SPF + SF	56	140	Geerts et al. (2018)
SC	SPI + pectin	55	120–140	Dekkers, Nikiforidis, et al. (2016)
SC	SPC	50–65	120–140	Grabowska et al. (2016)
TSE	PPI	60	140	Osen et al. (2015)
TSE	SPI + WG	50	148	Zhang et al. (2015)
TSE	SPI	50	150	Fang, Zhang, and Wei (2014)
SC	SPI + WG	70	95	Grabowska et al. (2014)
TSE	PPI	55	100–160	Osen et al. (2014)
SSE	PPC + DPF	50–55	165	Rehrah et al. (2009)
TSE	SPI + WG + WS	60–72	170	Liu and Hsieh (2008)

TSE, twin-screw extrusion; SC, shear cell; SSE, single screw extrusion; SPC, soy protein concentrate; MA, microalgae; PPI, pea protein isolate; WG, wheat gluten; PP, peanut protein; FPI, fababean protein isolate.; LPI, lupin protein isolate; SPI, soy protein isolate; CS, corn starch; SPF, soy protein fraction; SF, soy flour; WS, wheat starch; PPC, peanut protein concentrate; DPF, defatted peanut flour.

mixing and hydration of the ingredients and conveys them toward the end of the barrel. The screws can be equipped with different screw elements that induce more thorough mixing, such as kneading blocks (Figure 1*e*). The continuous mixing facilitates heat transfer, while the motion along the barrel results in a pressure build-up. The approximate pressure along the extruder barrel is presented in Figure 2. The high pressure prevents boiling of the material and allows for high processing temperatures. The combination of high shear and high temperature makes this a thermo-mechanical process. At the end of the barrel, pressure builds to a maximum as the material is pushed out of the barrel through the cone-shaped transition zone (Figure 1*f*). So-called breaker plates or diffusers (Figure 1*g*) can be placed before the cooling die, and are an often overlooked part of the extruder. Breaker plates are perforated steel disks that ensure a homogeneous pressure distribution and are thought to align the flow before it enters the cooling die (Cheftel, Kitagawa, and Queguiner 1992; Hine et al. 1997). The cooling die (Figure 1*h*) is a long rectangular channel and is cooled to a temperature of approximately 50 °C to ensure cooling and to prevent expansion of the extrudate when it exits the die (Figure 1*i*).

Shear cell

Shear cells were originally used as an off-line method to study the effect of extrusion-like conditions on biopolymers such as starch or proteins (Einde, Goot, and Boom 2003; Peighambardoust et al. 2004). When the processing of calcium caseinate led to the formation of fibrils (Manski, van der Goot, and Boom 2007b), the shear cell was identified as a novel structuring technology. The shear cell was later used as a new way of thermo-mechanical treatment (Grabowska et al. 2014). Contrary to HMEC, the process utilizes well-defined shear flow during heating. There are two types of shearing devices with either a cone-in-cone or a Couette design. The conical device is also known as the shear cell and consists of a stationary top cone (Figure 1*II*) and a rotating bottom cone (Figure 1*III*). The Couette device is a scale-up concept of the conical device and consists of a stationary outer cylinder and a rotating inner cylinder. These cylinders will induce Couette flow over the gap, similar to the shear flow inside the conical device.

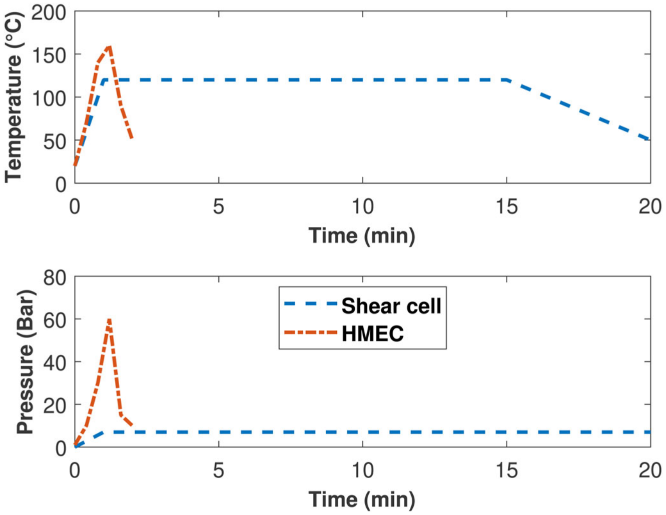

Figure 2. Comparison of the temperature and pressure profile during high-moisture extrusion cooking (HMEC) and shear cell processing. Values represent conventional process conditions as described by Cheftel, Kitagawa, and Queguiner (1992) for HMEC and Schreuders et al. (2019) for the shear cell.

The shear cell process has the same three basic unit operations as HMEC, being mixing and hydration, thermo-mechanical treatment, and cooling (Figure 1). A general procedure for dough preparation was identified. Most formulations use NaCl, which is first dissolved in water. A protein isolate or concentrate is mixed with the water (Figure 1*I*), either by hand with a spatula or using a Z-blade mixer, depending on the scale of operation (lab or pilot scale respectively). The water-protein mixture is left to hydrate

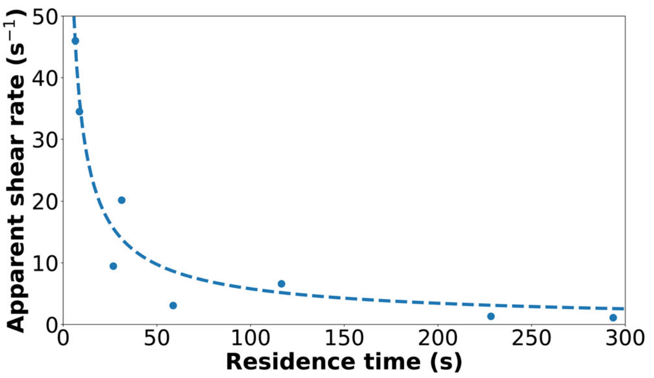

Figure 3. Apparent shear rate in the cooling die as calculated from the values from Table 2 (Equation 1 and 2) as a function of the residence time (Equations 2 and 3). The dotted line represents an exponential fit and serves to guide the eye ($\dot{\gamma}_{apparent} = 185\ t^{-0.75}$; $R^2 = 0.92$).

for 30 min at room temperature. After hydration, another protein or polysaccharide is added followed by further mixing to obtain a dough. The dough is transferred to the preheated shearing device and the shearing process is started.

Current versions of the conical shearing device rely on external heating by circulating heated water (Manski et al. 2008) or oil through the top and bottom cones (Grabowska et al. 2016). The use of oil enables high-temperature processing. The Couette device is heated by a steam jacket around the concentric cylinders (Krintiras et al. 2016). The shearing devices have seals and a pressurized cavity to prevent boiling and minimize moisture losses. This has enabled processing at conditions similar to extrusion cooking (Table 1; Figure 2; Grabowska et al. 2016; Dekkers, Nikiforidis, et al. 2016). A constant shear rate is applied to the material for 15 min while heating (conical device), resulting in thermo-mechanical treatment. The material is then cooled down by circulating cooled oil through the top and bottom cones of the shear cell. The shear cell is opened after the temperature reads 50 °C, which is low enough to solidify the material and avoid expansion due to the evaporation of water when opening the device. The bottom cone of the shear cell is stationary during cooling and, therefore, no shear rate is applied during cooling. Similarly, the Couette device is stationary while cooling.

Comparison of process conditions

Although the HMEC and shear cell processes are comparable in their basic unit operations, some differences can be noted. The main difference between HMEC and shear cell processing is that HMEC is a continuous process, while the shear cell process is batch-operated. Furthermore, the current shearing devices rely on external mixing (Figure 1*I*) and preparation of a dough, which is transferred to the preheated device (Krintiras et al. 2015, 2016; Grabowska et al. 2014). In HMEC the different ingredients are often fed to the extruder separately and mixed inside the barrel. Note that pre-mixing and hydration of ingredients can also be used in HMEC (Giezen, Jansen, and Willemsen 2014). The current window of operation for HMEC appears to be wider (100–175 °C) than for the shear cell (95–140 °C; Table 1). Moreover, the residence time of the HMEC process is much shorter at 2–5 min compared to at least 20 min for the conical shear cell (Figure 2).

Both during HMEC and shear cell processing a mechanical deformation is applied. Comparing the shear rates applied in both processes can be informative. The apparent shear in the shear cell is proportional to the rotation speed and is thus well defined. Although shear is applied in both the extruder barrel and the cooling die, not all shear is considered important for structure formation. The cooling die is often considered as the “structuring zone” (Figure 1*h*). Therefore, it is deemed more informative to only consider the shear rate in the cooling die here. The shear rate inside the cooling die is proportional to the die’s dimensions and the throughput, and can thus be calculated. Wall slip can occur in polymer melts when the wall shear exceeds a certain critical value (Hatzikiriakos 2012). The slip velocity is thought to depend on factors such as wall shear and normal stresses, temperature, and polymer properties such as the molecular weight distribution (Hatzikiriakos 2012). For simplicity, we have assumed a no-slip boundary in the die in our calculation of the apparent shear rate. The shear rate inside the die was calculated assuming no wall slip, after Son (2007):

$$\dot{\gamma}_{apparent} = 6 \cdot Q_{net}/(w \cdot h^2) \tag{1}$$

With $\dot{\gamma}_{apparent}$ as the apparent shear rate in the die, w the width and h the height of the die. The volumetric flow rate, Q_{net}, was calculated as:

$$Q_{net} = M/\rho_{melt} \tag{2}$$

With M as the mass feed rate. ρ_{melt} is the density of the melt and was approximated as 1087.2 kg m^{-3} by assuming a protein content of 40 wt%. The residence time in the die was calculated as:

$$t = V_{die}/Q_{net} \tag{3}$$

With V_{die} as the volume of the die calculated with $w \cdot h \cdot l$, in which l is the length of the die. The calculated shear rate in the cooling die ranges from 1 to 45 s^{-1} (Figure 3). There seems to be an exponential relation between residence time and shear rate, with processing at a low residence time resulting in higher apparent shear rates. This seems intuitive as a lower apparent shear rate would require a longer residence time to achieve a similar level of structure formation. Although most extrusion trials are based on empirical knowledge, there is probably a relation between the total shear applied and structure formation which is currently not well understood. During shear cell processing, a constant shear rate of 39 s^{-1} is most often applied, which is comparable to those used in low-throughput extrusion cooking (Figure 3). Other shear rates have also been used, namely 7–130 s^{-1} (Dekkers, Hamoen, et al. 2018). The total shear applied ($\gamma_{total} = \dot{\gamma}_{apparent} \cdot t$) in a shear cell is 3.5×10^4 when assuming a shear rate of 39 s^{-1} and a shearing time of 15 min. This is much higher than the total shear applied in the cooling die, which ranges from 1.8×10^2 to 7.7×10^2 (Table 2). We note that in a shear cell device the shear rate and pressure are independent from the throughput of the process,

Table 2. Overview of cooling die dimensions, process parameters, and apparent shear rates in the cooling die as calculated with Equations 1 and 2 during high-moisture extrusion cooking.

Mass feed rate (kg s^{-1})	*w* (m)	*h* (m)	*l* (m)	Apparent shear rate (s^{-1})	Reference
1.7×10^{-3}	7.0×10^{-2}	1.0×10^{-2}	5.0×10^{-2}	1.3	Samard, Gu, and Ryu (2019)
2.2×10^{-3}	5.0×10^{-2}	1.5×10^{-2}	8.0×10^{-1}	1.1	Palanisamy et al. (2019)
4.2×10^{-3}	3.0×10^{-2}	9.0×10^{-3}	3.8×10^{-1}	9.5	Pietsch et al. (2019)
7.2×10^{-3}	6.0×10^{-2}	1.0×10^{-2}	1.3	6.6	Caporgno et al. (2020)
6.7×10^{-4}	2.0×10^{-2}	2.0×10^{-3}	1.0×10^{-1}	4.6×10^{1}	Zhang et al. (2015)
5.0×10^{-4}	2.0×10^{-2}	2.0×10^{-3}	1.0×10^{-1}	4.5×10^{1}	Fang, Zhang, and Wei (2014)
2.8×10^{-4}	1.9×10^{-2}	2.0×10^{-3}	2.1×10^{-1}	2.0×10^{1}	Osen et al. (2014)
3.3×10^{-3}	6.0×10^{-2}	1.0×10^{-2}	3.0×10^{-1}	3.1	Liu and Hsieh (2008)

while these parameters are related for extrusion. The shear cell might, therefore, offer more flexibility in processing conditions.

Mixing and hydration

The first step in protein structuring is the mixing of the wet and dry ingredients to obtain a dough. In HMEC the raw materials are fed into the barrel and mixed through the continuous rotating motion of the screws (Figure 1*b*, *c*). The screws can exert high shear to the dough, especially at the screw tips where shear rates over 2430 s^{-1} were found according to the outcomes of computational fluid dynamics (CFD) simulations of starch matrices (Emin and Schuchmann 2013). The latter study also reported that the mixing index was highest when the shear rate was below 574 s^{-1}. This suggests that mixing is not proportional to the shear rate. The mixing processes used on lab and pilot scale versions of the shear cell may be more susceptible to lump formation due to the lower mixing intensity. Future industrial processing might cope with this by using twin-screw pre-mixers. Mixtures of different proteins, and proteins mixed with polysaccharides, do not tend to mix due to thermodynamic incompatibility (Grinberg and Tolstoguzov 1997; Tolstoguzov 1993; Polyakov, Grinberg, and Tolstoguzov 1997). Most HMEC and shear cell studies use moisture contents over 50% (Table 1). Upon hydration of a protein blend, the water will partition between the two phases. Clark et al. (1983) proposed the use of Time-Domain Nuclear Magnetic Resonance (TD-NMR) to study the water partitioning between proteins. TD-NMR was used to study the water partitioning in hydrated mixtures of soy protein and gluten (Dekkers, de Kort, et al. 2016), and pea protein and gluten (Schreuders et al. 2020). Both studies found that gluten binds less water than soy or pea protein. The water distribution was hardly affected after a thermo-mechanical treatment (95–140 °C and sheared at 39 s^{-1} for 15 min), as measured at room temperature (Dekkers, de Kort, et al. 2016; Schreuders et al. 2020). An alternative approach to determine the water partitioning is based on Flory-Huggins theory. Flory-Huggins theory describes the free energy of mixing polymers with a solvent, in this case, water. The free energy of mixing directly relates to the water activity. When the different polymer phases are in thermodynamic equilibrium, their water activities must be equal. Hence the equilibrium water distribution is found where the free energy is equal in both phases. Some proteins, such as gluten, form a cross-linked network. Stretching of the network during hydration will result in an additional elastic contribution to the free energy and must be taken into account by using Flory-Rehner theory instead. This approach was used to describe the water partitioning in mixtures of gluten with a protein isolate from either soy (Cornet, van der Goot, et al. 2020), pea, or fababean. Although the water distribution in polymer mixtures can be measured and predicted, the water distribution *during* thermo-mechanical treatment is currently unknown. This could be relevant for understanding structuring processes, as the rheological properties will be affected by the water distribution. It is still unclear whether the rheological properties of the dough are relevant for shear-induced structuring and the formation of anisotropic structures.

Thermo-mechanical treatment

The mixing and hydration step is followed by a thermo-mechanical treatment through the simultaneous application of heat and shear at elevated pressure (Figure 1). This combination of heat and shear is deemed essential as applying heat or shear alone does not result in a fibrous structure. The increase in temperature affects the intra- and intermolecular bonds that stabilize the protein structure. Hydrogen bonds are weakened as the temperature increases (Cordier and Grzesiek 2002), while hydrophobic interactions can increase with temperature (van Dijk, Hoogeveen, and Abeln 2015). Free thiol groups will become increasingly reactive as the temperature rises (Evans 2001), while preexisting intra- and intermolecular disulfide bonds become increasingly labile (Volkin and Klibanov 1987). Disulfide bonds can undergo alkali-catalyzed β-elimination to form free thiol groups; this reaction also occurs at neutral pH and high temperature (100 °C; Volkin and Klibanov 1987). Furthermore, free thiol groups and labile disulfide bonds can participate in thiol-disulfide interchange reactions to create a so-called transient or reversible network (Ryle and Sanger 1955; Bloksma 1975; Schofield et al. 1983). These thiol-disulfide interchange reactions may be promoted by shear stress (Evans 2001; Choi et al. 2007; Nagy 2013). The change in the protein's stabilizing interactions will result in a change or loss of the native protein structure, which is commonly referred to as denaturation. Most authors assume dense protein dispersions to reach a so-called molten state during thermo-mechanical treatment (Van Zuilichem 1992; Akdogan 1999; Zhang et al. 2019; Klüver and Meyer 2015; Osen et al. 2014; Pietsch, Emin, and Schuchmann 2017) due to the weakening of intra- and intermolecular interactions at high temperature. But while the formation of a melt is widely recognized, the properties of the protein melt and the effect of thermo-mechanical treatment on protein-protein interactions are subjects of debate. The different views will be discussed.

Wheat gluten and the fate of the disulfide bond

The interactions between proteins will greatly affect melt properties. Especially the disulfide bond is considered to play a pivotal role in melt properties and has been extensively studied for wheat gluten proteins (Strecker et al. 1995; Pietsch, Karbstein, and Emin 2018; Liu and Hsieh 2008; Lagrain, Thewissen, et al. 2008). Wheat gluten is a commonly used ingredient in both extruded and shear cell formulations (Table 1). The gluten proteins form a cross-linked network upon hydration (Ng and McKinley 2008; Attenburrow et al. 1990). The gluten network has the remarkable ability to be reversibly deformed beyond its breaking point. Bloksma (1975) proposed a mechanism to explain this behavior by assuming disulfide bonds to act as reversible cross-links at room temperature. Disulfide bonds can undergo what are known as thiol-disulfide interchanges, suggesting they could contribute to a reversible or *transient* network (Morel, Redl, and Guilbert 2002; Peressini et al. 2008; Peighambardoust et al. 2004; Edwards et al. 2001). Emin et al. (2017) showed that the complex modulus of gluten increases as the temperature exceeds 90 °C. This was attributed to the formation of glutenin polymers via disulfide bonding. Domenek et al. (2002) modeled the heat-induced aggregation of gluten proteins as a two-stage process ($T < 95\,^{\circ}C$), and concluded that the protein must first unfold before aggregating. Gluten aggregation is generally attributed to the formation of disulfide bonds (Domenek et al. 2002; Pietsch, Karbstein, and Emin 2018; Lagrain, Brijs, et al. 2008; Lagrain, Thewissen, et al. 2008). Schreuders et al. (2020) and Pietsch, Karbstein, and Emin (2018) measured the evolution of the viscoelastic properties of gluten in time at process-like conditions (100–160 °C). During iso-thermal experiments at a constant shear rate, both reported a maximum in the complex modulus and complex viscosity followed by a decrease. The maximum could hint toward cross-linking and aggregation, while the subsequent reduction could be due to a structural breakdown. The magnitude of, and time until the maximum was reached decreased with increasing temperature (Pietsch, Karbstein, and Emin 2018), which we suggest could be due to the weakening of the interactions with increasing temperature. This could be considered an indication of the presence of a transient network at higher temperatures. However, given the temporal evolution of the visco-elastic properties, it remains challenging to conclude what happens during thermo-mechanical processing of gluten inside the extruder barrel or shear cell. Emin et al. (2017) reported the evolution of the complex modulus as function of temperature (20–170 °C) for gluten hydrated to different levels (20, 30, 40%). The complex modulus decreased to a local minimum at ∼80–90 °C before reaching a maximum at 130–140 °C, and subsequently decreasing again. The increase was attributed to aggregation, while the decrease was attributed to structural break-down due to so-called degradation reactions. Whether reducing the temperature after heating over 130–140 °C restored the modulus was not reported, although it could have provided insight into the possibility of a transient network. A transient network would become permanent as the interactions become stronger at lower temperatures, leading to an increase in modulus. Interestingly, Emin et al. (2017) did refer to hydrated biopolymers at high temperatures as melts but did not consider melting as a result of weakened intermolecular interactions when interpreting the observed reduction in viscosity.

Disulfide bonding by non-gluten proteins

Understanding the fate of disulfide bonds in the melt is also important for other proteins. For soy protein it was shown that increasing the processing temperature over 130 °C leads to softening of the material, which was attributed to the partial breakdown of disulfide bonds (Shimada and Cheftel 1988). Dekkers, Boom, et al. (2018) studied the effect of temperature on soy protein isolate and showed a reduction in viscosity as the temperature exceeded 120–130 °C. Interrupting a time-sweep at high temperatures (120–140 °C) for 8 s resulted in a temporary increase in complex modulus, after which it returned to a similar magnitude as before the interruption. The increase in the complex modulus, ΔG^{*}, was lowest at 140 °C and was not affected by the time before interrupting the deformation. The protein network formed during the interruption was probably broken down again as soon as the deformation resumed, suggesting the presence of a transient network. At lower temperatures, ΔG^{*} was higher and increased with the time before interrupting. This could indicate that the material was not fully molten below 140 °C. Ralston and Osswald (2008) used a capillary rheometer to study the viscosity of bio-plastics based on soy protein and corn starch at 200 °C. They reported only a minor decrease in viscosity after repeatedly extruding the same sample at 200 °C. Similarly, Noguchi (1989) described how a fibrous soy extrudate could be cut up and extruded for a second and third time, while still resulting in a similar microstructure and fibrous texture. Dead-stop operation during re-extrusion indicated that the material had melted and fused together in the heated section of the barrel (Figure 1*d*; Noguchi 1989). O'Kane et al. (2004) showed that the elastic modulus of soy protein gels followed the same trajectory during reheating and subsequent cooling between 85 and 25 °C. For pea protein, they found that this could also be achieved when using a low initial cooling rate of $0.2\,^{\circ}C\ min^{-1}$. This suggests that the changes made to the gel network upon cooling are thermally reversible at these relatively low temperatures. Interestingly, Pietsch, Karbstein, and Emin (2018) reported no change in protein-protein interactions for soy protein isolate after processing at high temperature when compared to the raw material. Ingredient specific properties might, therefore, also be of importance. For example, the total number of cysteine residues differs between proteins and, therewith, also the number of potential disulfide bonds that can form.

Gluten contains relatively large amounts of cysteine (Shewry and Tatham 1997), while pea protein contains relatively low amounts. Berghout, Boom, and van der Goot (2015) studied the role of disulfide bonds in the gelation of protein isolates from lupin and soy. Lupin protein was found to contain more disulfide bonds and free thiol groups than soy protein. However, despite the higher number of potential disulfide bonds, lupin displayed poor gelling properties compared to soy. This was attributed to the large number of disulfide bonds on a single protein, which hindered protein unfolding and prevented gel formation. The accessibility of disulfide and free thiol groups is thus also of importance to network formation. Non-covalent physical interactions will also affect melt properties, especially for materials low in thiol groups and disulfide bonds.

Analysis of protein-protein interactions

Numerous studies have reported on the effect of thermal or thermo-mechanical treatment on the physical and covalent interactions between proteins. However, since most protein analyses can only be performed under ambient conditions, information on proteins *during* thermo-mechanical processing is limited. Many authors have, therefore, studied the material obtained *after* processing at elevated temperatures. A commonly used method to study the change in protein-protein interactions is by measuring protein solubility in different buffer systems (Samard, Gu, and Ryu 2019; Chiang et al. 2019; Zhang et al. 2020; Pietsch et al. 2019; Osen et al. 2015; Fang, Zhang, and Wei 2014; Liu and Hsieh 2007). The different buffers selectively disrupt the different types of protein-protein interactions, which is assumed to solubilize them. Phosphate buffers are often used to extract soluble proteins without disrupting any specific interactions. Urea is added to disrupt physical interactions such as hydrophobic-, ionic-, and hydrogen bonds. The addition of dithiothreitol (DTT) reduces the covalent disulfide bonds to free thiol groups (Liu and Hsieh 2007). Several authors have agreed that the extrusion of soy and pea protein at high temperatures leads to protein aggregation (Liu and Hsieh 2008; Chen, Wei, and Zhang 2011; Emin and Schuchmann 2017; Pietsch, Karbstein, and Emin 2018). The aggregates are thought to be due to a combination of covalent disulfide bonds and non-covalent physical bonds, although their relative importance is debated and will differ between protein sources. Interestingly, Pietsch et al. (2019) found that protein solubility in different buffer systems was not affected by thermo-mechanical treatment when compared to non-treated soy protein concentrate (SPC). From this, they concluded that the polysaccharide fraction of SPC must be responsible for the observed rheological changes. An alternative interpretation could be that the number of intermolecular interactions increased at a loss of intramolecular interactions. The use of buffer systems to determine protein–protein interactions is not without controversy. Liu and Hsieh (2008) showed that the buffer selection process is vital and that more conclusive results can be obtained by reversing the commonly used order of buffer addition. Instead of *adding* different reducing agents to the baseline buffer, they show that it could be better to *remove* reducing agents from a buffer system. This would allow for clearer differentiation between the relative importance of covalent and non-covalent bonds.

Another method to indirectly measure protein-protein interactions is based on the analysis of molecular weights before and after thermo-mechanical processing using sodium dodecyl sulfate–polyacrylamide gel electrophoresis (SDS-PAGE) (Chen, Wei, and Zhang 2011; Fang, Zhang, and Wei 2014; Osen et al. 2015; Zhang et al. 2020) or size exclusion chromatography (SEC) (Strecker et al. 1995; Domenek et al. 2002; Fang et al. 2013; Pietsch, Karbstein, and Emin 2018). Some authors observed a decrease in intensity of specific bands on the gel after extrusion of soy (Chen, Wei, and Zhang 2011, Chen et al. 2010; Fang, Zhang, and Wei 2014) and pea protein isolates (Osen et al. 2015). They attributed this to the formation of large aggregates that were unable to enter the gel's pores. Chen et al. (2010) also observed increased aggregation after raising the maximum temperature from 140 to 160 °C and after lowering the water content from 60 to 28% during the extrusion of soy protein. Fang, Zhang, and Wei (2014) reported an increase in low molecular weight fractions after the extrusion of soy protein. This further increased after raising the SME. In another study by the same author, extruded soy protein was again found to have higher fractions of low molecular weight components after extrusion, as determined using SEC and multi-angle laser light scattering (Fang et al. 2013).

So-called dead-stop experiments are often used to collect material from the different parts of an extruder (Chen, Wei, and Zhang 2011; Liu and Hsieh 2008; Yao, Liu, and Hsieh 2004). The extruder is simply shut-down when steady state is reached and left to cool before samples are taken. Liu and Hsieh (2008) performed dead-stop experiments and concluded that disulfide bonds are formed in the barrel as a result of high temperature and high moisture and that they do not change in the cooling die. However, in a dead-stop experiment samples are taken after cooling down the extruder and its contents. Similarly, the aforementioned studies on protein-protein interactions using buffer systems and size analysis methods have examined the material after cooling down. The findings from such studies may provide some insight into the material- and product properties, but cannot be used to elucidate the changes that occur *during* processing as the material changes upon cooling. Any changes invoked by the process can, therefore, not be attributed to a specific step in the process, be it heating, shearing, cooling, or a combination of those. Attributing specific functionality to a process step would facilitate the transition from empirical knowledge to a full understanding of thermo-mechanical structuring processes. Measurements at processing conditions are thus important and can be done either by measuring *inline* inside the extruder or shear cell, or by measuring *off-line* using dedicated analytical tools that mimic process conditions.

Barnes et al. (2007) reported on the use of several spectroscopic tools to study various melt properties during the processing of non-food polymers. They used Raman and Fourier Transform Near-Infrared spectroscopy (FT-NIR) to track melt compositions during the extrusion of ethylene-vinyl acetate. Huang et al. (2018) also used Raman spectroscopy to determine the ratio between polystyrene and polypropylene in the melt. Fluorescence spectroscopy was found to offer a real-time measure for the residence time during extrusion (Barnes et al. 2007). Hörmann et al. (2019) reported on the use of NIR spectroscopy during the extrusion of a pharmaceutical product. A fiber-optic probe located after the die section was used to monitor the concentration of the active pharmaceutical compound in the hot melt and to determine residence times. Hansen and Vedula (1998) reported on the use of NIR spectroscopy as an inline method to monitor the so-called melt index (MI) of polyethylene vinyl acetates. The MI is inversely proportional to the molecular weight and, at low stresses, also inversely proportional to the viscosity for synthetic polymers (Hansen and Vedula 1998). For some materials, spectroscopic tools could provide insight into both aggregation and viscosity. Although these tools have mostly been developed and used for non-food extrudates, they might also be used in food extrusion. In particular, Raman spectroscopy could prove insightful when studying protein melts. For example, disulfide bonds can be measured directly with Raman spectroscopy (Wang et al. 2016). Furthermore, the wavenumber is thought to vary between exposed and buried thiol groups (Ozakisj, Mizunolt, and Iriyamas 1987). Raman spectroscopy during thermo-mechanical treatment could, therefore, provide further insight into the fate of the disulfide bond. While spectroscopic tools can provide insight at the molecular level, other tools are needed to examine the rheological properties of the melt. The use of inline and off-line methodologies to study the rheological properties of the melt will be discussed in the next section.

Rheological characterization of the melt

Understanding how the viscous melt transforms into a fibrous product requires in-depth knowledge of the melt's rheological properties. However, obtaining meaningful rheological information is challenging as experimentally replicating the conditions found inside an extruder or shear cell is difficult (Emin et al. 2017; Dekkers, Emin, et al. 2018). Identifying the role of individual ingredients is complicated by factors such as water partitioning and changes in phase behavior. For example, Zhang et al. (2020) performed a rheological characterization of material collected from the different zones of an extruder by sampling after a dead-stop and re-dispersing the material in water at 20% (w/w). A molecular mechanism was postulated based on the viscosity curves determined at 25 °C to explain the extrudate properties. Such experiments may offer insight into the behavior of materials after processing. However, they do not necessarily relate to melt properties as they would occur during thermo-mechanical processing due to the change in temperature and moisture content. To achieve a better understanding of the phenomena during processing, well-designed experiments in which process-like conditions are used are essential. Two approaches were identified that are capable of measuring at relevant conditions. These analytical tools can either be incorporated into an extruder or shear cell to measure material properties *inline*, or they are external analytical tools that can mimic the process conditions to measure material properties *off-line*.

Inline rheological characterization

The use of inline rheometers, such as capillary or slit die rheometers, is considered the most accurate way to measure the viscosity of the melt (Thadavathi, Wassén, and Kádár 2019). Instead of an extrusion die, the slit die rheometer or capillary rheometer is attached to the end of the extruder. The pressure drop is measured over a section of known diameter and used to calculate the wall shear stress. The melt velocity is used to calculate the wall shear rate. By using several sections with a range of diameters in series an entire flow curve can be determined in a single run. A drawback of inline rheometers is that the change in diameter can modify back-pressure, which affects the degree of filling in the barrel. This could alter the thermo-mechanical stresses applied in the barrel (Emin et al. 2017). Therefore, it is crucial to keep the back-pressure constant. To achieve this, Horvat et al. (2013) designed an inline slit die rheometer with an adjustable geometry capable of maintaining a constant back-pressure, which ensures a constant processing history of the melt. Some studies successfully applied capillary rheometry to food materials and polymer melts (Corfield et al. 1999; Aichholzer and Fritz 1998; Ralston and Osswald 2008; Ponrajan et al. 2020; Beck et al. 2017).

Off-line rheological characterization

While inline methods offer direct measurements of material properties during processing, they are limited in their flexibility. Furthermore, inline methods also require operating an extruder at steady-state conditions. They are, therefore, unsuitable for ingredient screening and testing large numbers of samples. Off-line methods generally offer greater experimental flexibility and require smaller sample sizes. They are, therefore, better suited for small-scale testing and generating large data-sets. There are many different rheological tools available such as oscillatory shear rheometry, capillary rheometry and viscometry. These tools can be used to characterize ingredients and obtain information on material properties such as viscosity, elastic and viscous moduli, and elongational viscosity. However, most conventional bench-top rheometers are not capable of mimicking the high pressures, high temperatures, and high shear rates found during thermo-mechanical processing. Furthermore, preventing moisture losses is challenging when temperatures exceed 100 °C. Several manufacturers of bench-top rheometers do offer pressure cells for use with existing bench-top rheometers. The ability to perform rotational experiments and the greater torque sensitivity could prove advantageous as the viscosity of the protein melt is rather low (Schreuders et al. 2021).

Off-line capillary rheometers can also measure at high temperatures and pressure, and have been applied to study melt properties. Capillary rheometry is frequently applied in the field of plastic and bio-plastic extrusion. Klüver and Meyer (2015) reported on the shear and elongational viscosities of gluten, soy protein and pea protein, plasticized with glycerol at elevated temperatures ($T = 140$–$160\,^{\circ}\mathrm{C}$). The different protein melts were described as thermoplastic with shear-thinning behavior that could be approximated with power-laws with exponents of 0.31–0.40. Ralston and Osswald (2008) studied the shear viscosity of mixtures of soy protein and corn starch plasticized with glycerol and water. They also found shear-thinning and power-law behavior with comparable exponents. Extruding the material a second time resulted in a limited reduction in viscosity but did not affect the power-law exponent (Ralston and Osswald 2008). The limited effect of repeated thermo-mechanical treatment on the viscosity may explain why Noguchi (1989) was able to make fibers after repeated extrusion of defatted soy flour (Noguchi 1989). Food ingredients have also been studied using capillary rheometers. Beck et al. (2017) reported on the shear viscosity of hydrated pea protein isolate. They found that a longer holding time at 130 °C reduced the viscosity of pea protein isolate, although this effect was not significant. They suggested that the breakdown of aggregates over time could explain the observed trend. This appears to conflict with the notion that aggregation occurs at high temperature.

Closed cavity rheometry

A recent development is the use of rheometers that were originally designed for analyzing the vulcanization process of rubber compounds (Leblanc 2007; Mongruel and Cartault 2006; Hyun et al. 2011) for the rheological characterization of food polymers (Pommet et al. 2004; Emin et al. 2017; Pietsch et al. 2019; Geerts et al. 2018; Dekkers, Emin, et al. 2018; Schreuders et al. 2020). This class of rheometers has a closed cavity that can withstand high pressures and temperatures without the risk of evaporative moisture losses. In the field of food science these rheometers are, therefore, often referred to as "closed-cavity rheometers" or CCRs, as opposed to "rubber process analysers." CCRs can, to some degree, mimic the conditions inside a shear cell or extruder, although the accessible range of pressures and shear rates is limited. Furthermore, CCRs are not capable of rotation and can only impose an oscillatory deformation, which might limit the resemblance with the flow patterns that occur inside an extruder barrel or shear cell. By applying the Cox-Merz rule, the dynamic viscosities determined with a CCR could be used to determine the steady-state viscosities (Cox and Merz 1958). The principle of time-temperature superposition could also be used to create rheological master curves, as was demonstrated for cheese and whey proteins (Udyarajan, Horne, and Lucey 2007; Katsuta and Kinsella 1990). Rheological properties measured at higher temperatures may be described using for example the Carreau model (Allmendinger et al., 2014). Several pioneering studies have already employed CCRs to investigate the rheological properties of food polymers during thermo-mechanical treatment (Pommet et al. 2004; Geerts et al. 2018; Dekkers, Boom, et al. 2018; Schreuders et al. 2020; Pietsch, Karbstein, and Emin 2018, Pietsch et al. 2019). Some related this rheological fingerprint to the formation of a fibrous structure, as will be discussed in the "Mechanisms for structure formation" section. In addition to the CCR's intended purpose as a rheometric instrument, CCRs can be used as a method to produce samples for further analysis with other analytical methods. This could be particularly helpful when trying to separate the thermal and mechanical stresses during thermo-mechanical processing. In an extruder, the residence time is affected by the rotation speed of the screw inside the barrel. This limits and complicates the control over the duration and intensity of the thermal and mechanical stresses applied to the material. This issue is not there in shear cell processing, nor in the CCR. CCR rheometers can thus be used as a way to provide thermo-mechanical treatment to samples in a controllable way, as has been done by Pietsch, Karbstein, and Emin (2018). The application of CCRs for the analysis of food polymers and food polymer melts is still in its infancy and dedicated CCRs capable of more accurately mimicking extrusion-like conditions may yet be developed.

In the context of food, some consider the extruder barrel as a chemical reactor in which thermo-mechanical stresses induce changes in the material (Pietsch, Karbstein, and Emin 2018; Emin et al. 2017). In particular, the cross-linking of gluten has been studied extensively in this regard. Morel, Redl, and Guilbert (2002) showed that shear can reduce the activation energy required to induce gluten cross-linking below 80 °C. Similarly, Strecker et al. (1995) used an extrusion rheometer to show that gluten polymerization speeds up with the shear rate (40–170 °C). We must note that the activation energy for cross-linking reported by Strecker et al. (1995) is approximately 5–10 times lower than the value found in a more recent study by Domenek et al. (2002). The lowering effect of shear on the activation energy suggests that shear can facilitate the interaction between proteins. The reduced activation energy could relate to the concept of effective temperature. This concept suggests that the viscous forces can increase the effective temperature of the system and thereby lower the energy barrier of a reaction. This might explain the importance of shear during thermo-mechanical treatment. Emin and Schuchmann (2017) showed that an increase in shear rate during iso-thermal processing of gluten in a CCR reduced the complex viscosity ($T = 120\,^{\circ}\mathrm{C}$; $\dot{\gamma} = 0.1$–$50\,\mathrm{s}^{-1}$). Interestingly, in a similar experiment Pietsch, Karbstein, and Emin (2018) did not find an effect of increasing the shear rate from 0.1 to $50\,\mathrm{s}^{-1}$ on the amount of SDS-soluble gluten proteins for a range of temperatures. Similarly, the processing of soy protein concentrate (SPC) in a CCR at different shear rates did not result in significant changes in protein solubility across a range of extraction buffers (Pietsch et al. 2019). This suggests that food protein cross-linking may not be a thermo-mechanical but merely a thermal process at lower shear rates. At the higher shear rates cross-linking could still be affected. Noguchi (1989) showed that the repeated extrusion of defatted soy progressively reduced the soluble protein fractions while getting a fibrous structure after all three passes through the extruder. They, therefore, argued that "texturization" and "reactions" such as cross-linking should be considered as separate (Noguchi 1989).

The use of large amplitude oscillatory shear (LAOS) rheology as well as the energy dissipation ratio, which shows a simplified perspective to reveal the complex information in the Lissajous curve, have also been picked up as tools to study melt properties (Schreuders et al. 2021). LAOS provides information on the rheological properties beyond the linear viscoelastic regime but is more difficult to interpret than conventional small amplitude oscillatory shear (SAOS) measurements (Hyun et al. 2011). Using LAOS methods it was found that a thermal treatment can increase the elasticity of protein networks (Schreuders et al. 2021). The thermal treatment caused pea protein isolate to lose its elastic properties more quickly than soy protein isolate and gluten.

The identification of new rheological tools has enabled the determination of rheological properties of the melt. This has led to rheological fingerprinting of the melt. A next step will be to understand and interpret these complex results and relate them to the structuring process.

Cooling

After the thermo-mechanical treatment, the melt is cooled down (Figure 1). Cooling leads to a strengthening of the non-covalent interactions and the labile disulfide bonds become permanent ("Thermo-mechanical treatment" section). This first results in an increase in viscosity before the material fully solidifies and the structure is fixed. When assuming the presence of a transient network in the melt, this network will become permanent upon cooling. An additional purpose of cooling is to prevent the expansion of the product as it exits the die or after opening the shear cell. Since the melt is cooled from the outside a viscosity gradient will be present before the material is fully solidified, with a lower viscosity in the hot interior. The significance of this change in viscosity depends on whether shear is applied during cooling.

The solidified material will have formed a cross-linked polymer network or gel. The protein source and concentration, cooling rate and heating temperature all affect the gel's properties. For example, pea protein isolates form weaker and less elastic gels compared to soy protein isolate (Lam et al. 2018; O'Kane et al. 2004). O'Kane et al. (2004) showed that a low cooling rate results in stronger gels for both pea legumin and soy glycinin by measuring the storage modulus. Transmission electron microscopy showed more branched networks for samples made with a low cooling rate. This was attributed to the proteins remaining unfolded for longer, allowing for interactions and disulfide bonds to form more optimally (O'Kane et al. 2004). However, it is unclear whether these findings also apply to the gelation during thermo-mechanical processing. Liu and Hsieh (2007) compared heat-induced gels with extrudates made from SPI. Extrudates were found to be around 10 times harder and to have more disulfide bonds as measured via buffer extraction. However, since the gels were prepared at a much lower temperature (95 °C) than the extrudates (170 °C), direct comparison of these results is difficult. Apart from the cooling rate, also the protein concentration influences the modulus of SPI gels, with a higher concentration resulting in a higher modulus (Cornet, van der Goot, et al. 2020).

Mechanisms for structure formation

Now that we have described the different unit operations commonly found in thermo-mechanical processes and the effects they have on the material, we can discuss the mechanism behind the structure formation itself. Since HMEC has been studied for a longer time than the shear cell, it is not surprising that effectively all hypotheses on structure formation stem from HMEC. Most mechanisms consider the cooling die (Figure 1*h*) as the "structuring zone" where the formation of the fibrous structure takes place (Akdogan 1999; Tolstoguzov 1993; Cheftel, Kitagawa, and Queguiner 1992; Sandoval Murillo et al. 2019). However, the structuring zone may extend toward other regions of the extruder as well (Yao, Liu, and Hsieh 2004; Lin and Cheung 1997). All the identified mechanisms assume the presence of multiple phases that are in relative motion. However, they differ in the assumed reason for the multi-phase system, or the origin of the relative motion. As mentioned, these mechanisms have been developed with HMEC in mind. However, the proposed mechanisms may still apply to both HMEC and shear cell processing given the similar conditions inside (the beginning of) a cooling die and a heated, rotating shear cell. An overview of the different mechanisms is presented in Table 3 alongside a schematic representation of the mechanisms.

Phase behavior of protein mixtures

The presence of two (or more) separate phases in bio-polymer mixtures is broadly accepted and has been studied extensively using a range of experimental and theoretical tools (Grinberg and Tolstoguzov 1997; Polyakov, Grinberg, and Tolstoguzov 1997; Tolstoguzov 1993; Cheftel, Kitagawa, and Queguiner 1992; Grabowska et al. 2014; Dekkers, de Kort, et al. 2016; Schreuders et al. 2020; Cornet, van der Goot, et al. 2020). The group of Tolstoguzov showed that protein-polysaccharide mixtures generally tend to phase-separate (Grinberg and Tolstoguzov 1997; Tolstoguzov 1993), and that protein-protein blends do not mix at concentrations relevant to extrusion and shear cell processing (Polyakov, Grinberg, and Tolstoguzov 1997). Some do consider the hot melt as homogeneous, with separation occurring upon cooling down (Ledward and Tester 1994; Sandoval Murillo et al. 2019). However, the presence of two separate phases in bio-polymer mixtures was confirmed experimentally for hydrated mixtures of soy protein and gluten. The use of TD-NMR and rheological methods led to

Table 3. Schematic representation of different structuring mechanisms that could be responsible for the structuring potential of plant-proteins.

Mechanism	Applicability	Schematic representation
Laminar flow results in a velocity gradient, which induces fiber formation parallel to the deformation. Velocity gradients can be enhanced by temperature-induced viscosity gradients (Akdogan 1999, Cheftel, Kitagawa, and Queguiner 1992)	HMEC	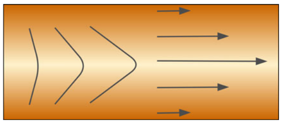
Phase deformation and alignment, the dispersed phase in the melt is deformed in the flow direction (Tolstoguzov 1993)	HMEC, SC	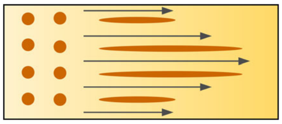
Elongational flow in the breaker plate, the dispersed phase is deformed in the flow direction while passing through the breaker plate (Hine et al. 1997)	HMEC	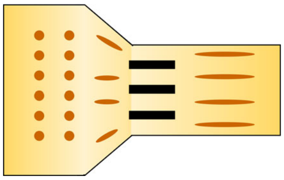
Spinodal decomposition, the homogeneous melt undergoes spinodal deformation into a water-rich and water-poor phase as a result of shear and a critical cooling temperature (Sandoval Murillo et al. 2019)	HMEC	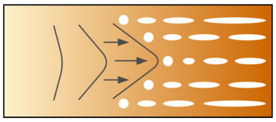

HMEC, high-moisture extrusion cooking, SC, shear cell.

the insight that at both 25 °C (Dekkers, de Kort, et al. 2016) and 140 °C two separate phases are present (Schreuders et al. 2020).

Dekkers, Emin, et al. (2018) studied the rheological properties of soy protein and gluten. They suggested that to create fibrous structures the two phases in a bio-polymer mixture must have similar rheological properties during processing at high temperature. Schreuders et al. (2020) later showed that pea protein and gluten have rather different rheological properties but can still be fibrillated. The similarity in rheological properties of the two phases, therefore, does not seem to be a universal requirement. Grabowska et al. (2014) showed that gluten alone can form fibrous structures in the shear cell. Adding up to 50% of another protein (soy, pea, fababean) still resulted in the formation of fibers. It was suggested that gluten should be a continuous phase, and is primarily responsible for fiber formation in gluten-containing mixtures. The second protein may act merely as a filler and may thus be easily replaced.

Protein isolates are multi-protein ingredients but are often assumed to behave as a single-phase when molten. This suggests that multiple ingredients are needed to obtain a two-phase system. Interestingly, the formation of fibrous structures from a single-ingredient has also been reported, such as through extrusion of hydrated pea protein isolate (Osen et al. 2015) or soy protein isolate (Fang, Zhang, and Wei 2014). Arêas (1992) proposed that single-ingredient systems can still behave as a two-phase system. They described in an earlier study that insoluble and non-melting components in a protein isolate could act as a second phase and induce structure formation. Indeed, the polysaccharides in protein concentrates can also act as a second phase (Grabowska et al. 2016). Hydrated gluten is also thought to form a two-phase system due to partitioning based on the molecular weight (Boire et al. 2013). This might explain why processing hydrated gluten in a shear cell results in a fibrous product (Grabowska et al. 2014. Despite the predominant thought that protein melts are multi-phase systems, a recent paper by Sandoval Murillo et al. (2019) posed that the hot melt is a homogeneous single-phase system of hydrated bio-polymers. They hypothesized that a melt of pea protein isolate and water decomposes into water-rich and protein-rich domains upon entering the cooling die due to *spinodal decomposition*. The spinodal decomposition of the melt in the die section was simulated using the Cahn-Hilliard equation. Phase separation was assumed to be temperature-driven through a temperature-dependent free-energy. The notion of a homogeneous, single-phase melt seems to conflict with the often assumed thermodynamic incompatibility of proteins. Protein isolates are always mixtures of different proteins despite originating from the same crop, in this case, pea. Different phases could, therefore, still be a possibility. Furthermore, as also stated by Sandoval Murillo et al. (2019), some of the used model parameters such as the chosen interfacial tension, may not have been appropriate. Regardless, they provide an interesting hypothesis for structure formation in the die.

Flow-induced structuring mechanisms

All the identified hypotheses for structure formation consider the importance of the flow behavior of the melt. The Reynolds number, *Re*, can give insight into flow behavior by providing an indication of whether laminar (low *Re*) or turbulent flow (high *Re*) could be expected. When assuming a rectangular duct, the Reynolds number can be calculated as (Metzner and Reed 1955):

$$Re = \frac{\rho_{melt} \cdot u \cdot D_H}{\mu} \tag{4}$$

With ρ_{melt} as the melt density (1087.2 kg m^{-3}), u as the average melt velocity, and μ as the melt dynamic viscosity. The hydraulic diameter, D_H, was calculated as $D_H = \frac{4 \cdot A}{C}$ with A as the cross-sectional area and C as the circumference of the die. When assuming a melt viscosity of 1 kPas, the Reynolds numbers for the processes in Table 1 range from 2 to 73. At such low Reynolds numbers, it is reasonable to assume laminar flow (Metzner and Reed 1955). The *laminar flow* profile in the cooling die is often considered to be responsible for structure formation (Zhang et al. 2019; Akdogan 1999; Osen et al. 2014; Palanisamy et al. 2019; Sandoval Murillo et al. 2019). However, the type of laminar flow is most often not specified, although some have assumed shear flow at the entrance of the die and plug flow toward the end of the die (Sandoval Murillo et al. 2019). Shear flow has been shown to induce alignment in dilute polymer solutions when flowing through a rectangular or circular die (Mitsoulis 2010). Cheftel, Kitagawa, and Queguiner (1992) and later Akdogan (1999) discussed a mechanism where the melt would solidify as it passes through the cooling die. The material closest to the die wall would be cooled down first and, therefore, increase in viscosity. The interior would remain hotter and, therefore, of lower viscosity. The difference in viscosity would enhance the velocity gradient in the cooling die. This was suggested as the origin of fiber formation. While the mechanism hypothesized by Cheftel, Kitagawa, and Queguiner (1992) and Akdogan (1999) is commonly considered reasonable, direct proof in support of the hypothesis is limited to visual observations of the extrudate (Cheftel, Kitagawa, and Queguiner 1992). Future research could combine rheological measurements with modeling to test this hypothesis further.

The group of Tolstoguzov showed that the dispersed phase in emulsions can be deformed by shear flow. The degree of droplet deformation was found to depend on the viscosity ratio between the two phases (Tolstoguzov, Mzhel'sky, and Gulov 1974). They also studied the extrusion of bio-polymer mixtures (Tolstoguzov 1993; Grinberg and Tolstoguzov 1997; Polyakov, Grinberg, and Tolstoguzov 1997). The mechanism they proposed for the deformation of emulsion droplets was also used to explain structure formation inside the cooling die during low-moisture extrusion (Tolstoguzov 1993). It was assumed that droplets of the dispersed phase *deform and align* in the shear flow direction (Table 3). Individual droplets could coalesce and result in both long and short fibers. The low interfacial tension between phases in water-in-water emulsions would facilitate the generation of the additional interface and facilitate phase deformation and alignment (Tolstoguzov 1993). The formed structure could be fixed through cooling. This mechanism has been applied by Dekkers, Nikiforidis, et al. (2016) to explain the formation of a fibrous structure obtained after processing soy protein isolate and citrus pectin in a shear cell. Soy can also act as a co-continuous or dispersed phase when combined with gluten (Schreuders et al. 2020). The continuous phase may thus depend on the combination of ingredients used. If the mechanism posed by Tolstoguzov (1993) would apply to a bi-continuous system is unclear.

Barrel to die transition zone

While most authors have focused on the cooling die when studying structure formation, the section between the barrel and the cooling die could also be of importance to the structure formation process. Yao, Liu, and Hsieh (2004) used dead-stop experiments to study structure formation inside the barrel using soy protein, gluten and starch. Their results showed that fiber formation may start at the end of the barrel as indicated by both an increase in anisotropy and visual inspection of the structure. However, as also mentioned in the original study, the dead-stop approach could have affected the structure.

In the transition zone between the barrel and the cooling die, a so-called breaker plate can be present (Figure 1*g*). The breaker plate can homogenize the pressure and pre-align the flow before the melt enters the cooling die. Hine et al. (1997) studied the effect of removing the breaker plate on the alignment of glass fiber in reinforced polypropylene extrudates. The use of a breaker plate resulted in more alignment of the glass fibers, which was attributed to the pre-alignment of the fibers by the breaker plate. Lin and Cheung (1997) reported the presence of strands inside the extrudates when extruding blends of polyoxymethylene (POM) and polypropylene (PP). The location and positioning of the strands matched the holes of the breaker plate. Probably, the spherically shaped dispersed phase experienced *elongational flow* when passing through the breaker plate. This could have stretched the dispersed phase into elongated strands, resulting in the observed structure. Local concentrations of the two polymers varied, with the outer strands higher in polypropylene. Although one of the main purposes of a breaker plate is to stabilize and align the flow, their potentially significant role in structure formation has to our knowledge not yet been picked up in the field of food science.

Shear-induced structuring in some non-food systems

Foods can be considered highly complex in both composition and behavior. This complexity can hinder the elucidation of the underlying mechanisms by impeding direct measurements and obscuring the behavior. It can, therefore, be of interest to study systems that are simpler in terms of composition. Shear-induced structure formation is also seen in particle suspensions and two-phase polymer systems. We will discuss some of the findings from these fields and discuss their potential implications for the thermo-mechanical processing on foods.

Flow-induced structure formation is frequently observed in suspension rheology in the form of shear-bands (Scirocco, Vermant, and Mewis 2004; Pasquino et al. 2010; Van Loon et al. 2014; Santos De Oliveira et al. 2011; Divoux et al. 2016; Vermant and Solomon 2005). Van Loon et al. (2014) systematically investigated the importance of several rheological characteristics of the continuous phase for the occurrence of shear bands and identified shear-thinning behavior of the continuous phase as essential for the formation and stability of shear-bands. As two particles approach each other, the local shear rate will increase. This would locally reduce the viscosity of the shear-thinning fluid, and limit the hydrodynamic coupling between particles. This, they argue, would enable each particle on the chain to satisfy the zero-torque condition, and thus keep the chain as a whole from tumbling and breaking up. The resemblance between a shear-thinning fluid with dispersed rigid particles and a two-phase polymer melt may be limited. Polymer melts are generally shear-thinning, which suggests that both the continuous and dispersed phases of the melt will have similar properties. However, the properties of the dispersed phase may not be comparable to those of the relatively rigid colloidal particles used in the aforementioned studies. Although approximating the dispersed phase as rigid particles may be an over-simplification, some of the physics may still apply. Whether shear-thinning of the continuous phase is decisive for structure formation in HMEC or shear cell processing thus remains unclear.

The formation of shear-bands has also been observed in sheared polymer solutions (Caserta and Guido 2012; Cromer et al. 2013; Caserta, Simeone, and Guido 2008; Migler 2001). Caserta, Simeone, and Guido (2008) showed that a mixture of two immiscible polymer solutions can form shear-bands (Caserta, Simeone, and Guido 2008). Shear-band formation was associated with a reduction in overall viscosity of the system and is, therefore, thought to be an effort of the system to reduce the viscous energy dissipation (Caserta, Simeone, and Guido 2008). The droplets present in solutions of two immiscible polymers can also align on a string parallel to the flow direction (Migler 2001; Caserta, Simeone, and Guido 2008). When the viscosity ratio was reduced to 0.01, droplets formed "pearl-necklace" structures parallel to the vorticity direction superimposed to those in the flow direction (Caserta, Simeone, and Guido 2008). The dimensionless size of the droplets was shown to scale with the dimensionless shear rate, until a transition from droplets to string formation occurred as the shear rate went below $2.5\,\mathrm{s}^{-1}$ (Migler 2001). Moving through this transition induces a change in microstructure from individual droplets to elongated strings through alignment and coalescence of the individual droplets.

Most of these studies use semi-dilute polymer solutions (10% vol/vol); much lower concentrations than commonly used in food extrusion (>30 wt%). Still, some similarities can be identified. The observations by Migler (2001) for dilute two-phase polymer solutions are comparable to the mechanism proposed by Tolstoguzov (1993) for extrudates.

General discussion

We have reviewed the thermo-mechanical processing of plant-proteins through HMEC and shear cell processing for the production of plant-based meat analogues. The HMEC and shear cell processes were found to be comparable in their basic processing steps. These steps are mixing and hydration, thermo-mechanical treatment, and cooling (Figure 1). We noticed a lack of understanding of the physical changes that are induced by the process, most notably the effect of thermo-mechanical treatment on protein-protein interactions. Furthermore, the mechanism by which fibrous structures are made remains unclear.

The effect of thermo-mechanical treatment on proteins has been studied extensively. However, many studies focused on the product obtained *after* processing. While this may provide insight into product properties, it does not provide conclusive information on protein behavior *during* processing. Indeed, direct measurement of for example protein-protein interactions at processing conditions is challenging with the currently available machinery. However, it is our opinion that thermo-mechanical processes can only be fully understood by learning the nature of protein-protein interactions at the relevant processing conditions. The use of inline spectroscopic methods such as NIR and Raman spectroscopy could greatly improve our understanding of the behavior of proteins during thermo-mechanical processing.

We identified several hypotheses to explain the formation of fibrous structures. These hypotheses are all based on flow-induced deformation (Table 3). Due to the lack of shear during cooling in the shear cell process, structure formation in shear cell processing is expected to be completed as soon as the shear is stopped. The mechanisms that assume shear during cooling (spinodal decomposition and deformation; temperature-induced viscosity gradients; Table 3), therefore, cannot apply to the shear cell. The mechanism of a deformed dispersed phase could apply to both structuring processes. However, the amount of direct evidence supporting the different mechanisms is limited and keeps us from selecting a universal mechanism for the thermo-mechanical structuring of plant proteins. Furthermore, we found that the often overlooked breaker plates found in extruders could play an important role in structure formation by providing elongational flow. Moreover, the fact that fibrous structures can be made from ingredients with different properties suggests that different mechanisms may result in a similar fibrous product. Therefore, more direct and indirect measurements of material properties inside the cooling die and shear cell are necessary to confirm the mechanism underlying structure formation. For example, the shear cell developed by Velichko et al. (2019) combined with (ultra-) small-angle neutron and X-ray scattering (SANS/SAXS) could provide insight into the micro- and nano-scale structure of flowing two-phase systems. Doppler Velocimetry (Münstedt and Schwarzl 2014) could prove useful by providing an inline measurement of the flow profile. Furthermore, the extensive body of work on flow-induced structuring in non-food suspensions and polymer mixtures and future studies using simplified model systems could provide further insight.

Off-line methodology will also play an important role due to their flexibility and ease of operation. The use of sophisticated closed-cavity rheometers (CCRs) could mark the start of a revolution in protein structuring as they enable measuring rheological properties at high temperatures and pressures. However, the currently available CCRs cannot match all of the relevant process conditions such as pressure and shear rate. Therefore, the development of CCRs dedicated to protein melt analysis may be necessary. These devices should include the ability to perform rotational experiments in addition to oscillatory experiments to improve the resemblance with thermo-mechanical processing. The additional insight into material properties during processing could be used as an input for physical model simulations. Accurate model inputs are essential to the validity of simulation results. While models are always simplifications of reality, they could help in identifying the relevant process parameters and could limit the number of extrusion or shear cell trials needed to answer a specific research question.

In conclusion, we have found that thermo-mechanical processing still has many open questions. These questions will need to be answered through the use of online and off-line methods to obtain better control over the process, and to ultimately acquire predictive power concerning ingredient–product relationships.

Acknowledgment

We acknowledge Irene Meulensteen for her help in identifying the breaker plate as a component of interest.

Disclosure statement

There are no competing interests to declare.

Funding

This work was part of the projects Plant Meat Matters, and PlantPromise, both co-financed by the Top Consortium for Knowledge and Innovation Agri & Food by the Dutch Ministry of Economic Affairs under contract numbers TKI-AF-16011 and LWV-19027 respectively, and the project GreenXProt, co-financed by the Swiss Innovation Agency "Innosuisse" under contract number 36440.1 IP-LS.

ORCID

Steven H. V. Cornet http://orcid.org/0000-0002-6304-4508
Silvia J. E. Snel http://orcid.org/0000-0001-9751-2229
Floor K. G. Schreuders http://orcid.org/0000-0001-8051-8173
Ruud G. M. van der Sman http://orcid.org/0000-0003-4964-0247

References

Aichholzer, W., and H. G. Fritz. 1998. Rheological characterization of thermoplastic starch materials. *Starch - Stärke* 50 (2–3):77–83. doi: 10.1002/(SICI)1521-379X(199803)50:2/3 < 77::AID-STAR77 > 3.0.CO;2-P.

Aiking, H., and J. de Boer. 2020. The next protein transition. *Trends in Food Science and Technology* 105:515–22. doi: 10.1016/j.tifs.2018.07.008.

Akdogan, H. 1999. High moisture food extrusion. *International Journal of Food Science & Technology* 34 (3):195–207. doi: 10.1046/j.1365-2621.1999.00256.x.

Allmendinger, A., S. Fischer, J. Huwyler, H. C. Mahler, E. Schwarb, I. E. Zarraga, and R. Mueller. 2014. Rheological characterization and injection forces of concentrated protein formulations: An alternative predictive model for non-Newtonian solutions. *European Journal of Pharmaceutics and Biopharmaceutics* 87 (2):318–28. doi: 10.1016/j.ejpb.2014.01.009.

Arêas, J. 1992. Extrusion of food proteins. *Critical Reviews in Food Science and Nutrition* 32 (4):365–92. doi: 10.1080/10408399209527604.

Attenburrow, G., D. J. Barnes, A. P. Davies, and S. J. Ingman. 1990. Rheological properties of wheat gluten. *Journal of Cereal Science* 12 (1):1–14. doi: 10.1016/S0733-5210(09)80152-5.

Barnes, S. E., M. G. Sibley, H. G. M. Edwards, and P. D. Coates. 2007. Process monitoring of polymer melts using in-line spectroscopy. *Transactions of the Institute of Measurement and Control* 29 (5):453–65. doi: 10.1177/0142331207084336.

Beck, S. M., K. Knoerzer, J. Sellahewa, M. A. Emin, and J. Arcot. 2017. Effect of different heat-treatment times and applied shear on secondary structure, molecular weight distribution, solubility and rheological properties of pea protein isolate as investigated by capillary rheometry. *Journal of Food Engineering* 208:66–76. doi: 10.1016/j.jfoodeng.2017.03.016.

Berghout, J. A. M M., R. M. Boom, and A. J. van der Goot. 2015. Understanding the differences in gelling properties between lupin protein isolate and soy protein isolate. *Food Hydrocolloids* 43:465–72. doi: 10.1016/j.foodhyd.2014.07.003.

Bloksma, A. H. 1975. Thiol and disulfide groups in dough rheology. *Cereal Chemistry* 52 (3):170–83.

Boire, A., P. Menut, M. H. Morel, and C. Sanchez. 2013. Phase behaviour of a wheat protein isolate. *Soft Matter* 9 (47):11417–26. doi: 10.1039/c3sm51489g.

Campbell, M. F. 1981. Processing and product characteristics for textured soy flours, concentrates and isolates. *Journal of the American Oil Chemists' Society* 58 (3 Part 2):336–8. doi: 10.1007/BF02582372.

Caporgno, M. P., L. Böcker, C. Müssner, E. Stirnemann, I. Haberkorn, H. Adelmann, S. Handschin, E. J. Windhab, and A. Mathys. 2020. Extruded meat analogues based on yellow, heterotrophically cultivated Auxenochlorella protothecoides microalgae. *Innovative Food Science & Emerging Technologies* 59:102275. doi: 10.1016/j.ifset.2019.102275.

Caserta, S., and S. Guido. 2012. Vorticity banding in biphasic polymer blends. *Langmuir* 28 (47):16254–62. doi: 10.1021/la303232w.

Caserta, S., M. Simeone, and S. Guido. 2008. Shear banding in biphasic liquid-liquid systems. *Physical Review Letters* 100 (13):137801–4. doi: 10.1103/PhysRevLett.100.137801.

Chaudhary, A., D. Gustafson, and A. Mathys. 2018. Multi-indicator sustainability assessment of global food systems. *Nature Communications* 9 (1):848. doi: 10.1038/s41467-018-03308-7.

Cheftel, J. C., M. Kitagawa, and C. Queguiner. 1992. New protein texturization processes by extrusion cooking at high moisture levels. *Food Reviews International* 8 (2):235–75. doi: 10.1080/87559129209540940.

Chen, F. L., Y. M. Wei, and B. Zhang. 2011. Chemical cross-linking and molecular aggregation of soybean protein during extrusion cooking at low and high moisture content. *LWT - Food Science and Technology* 44 (4):957–62. doi: 10.1016/j.lwt.2010.12.008.

Chen, F. L., Y. M. Wei, B. Zhang, and A. O. Ojokoh. 2010. System parameters and product properties response of soybean protein extruded at wide moisture range. *Journal of Food Engineering* 96 (2):208–13. doi: 10.1016/j.jfoodeng.2009.07.014.

Chiang, J. H., S. M. Loveday, A. K. Hardacre, and M. E. Parker. 2019. Effects of soy protein to wheat gluten ratio on the physicochemical properties of extruded meat analogues. *Food Structure* 19:100102. doi: 10.1016/j.foostr.2018.11.002.

Choi, H., K. Aboulfatova, H. J. Pownall, R. Cook, and J. F. Dong. 2007. Shear-induced disulfide bond formation regulates adhesion activity of von Willebrand factor. *The Journal of Biological Chemistry* 282 (49):35604–11. doi: 10.1074/jbc.M704047200.

Clark, A. H., R. K. Richardson, S. B. Ross-Murphy, and J. M. Stubbs. 1983. Structural and mechanical properties of agar/gelatin co-gels. Small-deformation studies. *Macromolecules* 16 (8):1367–74. doi: 10.1021/ma00242a019.

Cordier, F., and S. Grzesiek. 2002. Temperature-dependence of protein hydrogen bond properties as studied by high-resolution NMR. *Journal of Molecular Biology* 317 (5):739–52. doi: 10.1006/jmbi.2002.5446.

Corfield, G. M., M. J. Adams, B. J. Briscoe, P. J. Fryer, and C. J. Lawrence. 1999. A critical examination of capillary rheometry for foods (exhibiting wall slip). *Food and Bioproducts Processing* 77 (1): 3–10. doi: 10.1205/096030899532196.

Cornet, S. H. V., A. J. van der Goot, and R. G. M. van der Sman. 2020. Effect of mechanical interaction on the hydration of mixed soy protein and gluten gels. *Current Research in Food Science* 3:134–45. doi: 10.1016/j.crfs.2020.03.007.

Cox, W. P., and E. H. Merz. 1958. Correlation of dynamic and steady flow viscosities. *Journal of Polymer Science* 28 (118):619–22. doi: 10.1002/pol.1958.1202811812.

Cromer, M., M. C. Villet, G. H. Fredrickson, and L. G. Leal. 2013. Shear banding in polymer solutions. *Physics of Fluids* 25 (5): 051703–7. doi: 10.1063/1.4805089.

Dekkers, B. L., C. V. Nikiforidis, and A. J. van der Goot. 2016. Shear-induced fibrous structure formation from a pectin/SPI blend. *Innovative Food Science & Emerging Technologies* 36:193–200. doi: 10.1016/j.ifset.2016.07.003.

Dekkers, B. L., D. W. de Kort, K. J. Grabowska, B. Tian, H. Van As, and A. J. van der Goot. 2016. A combined rheology and time domain NMR approach for determining water distributions in protein blends. *Food Hydrocolloids* 60:525–32. doi: 10.1016/j.foodhyd.2016.04.020.

Dekkers, B. L., M. A. Emin, R. M. Boom, and A. J. van der Goot. 2018. The phase properties of soy protein and wheat gluten in a blend for fibrous structure formation. *Food Hydrocolloids* 79:273–81. doi: 10.1016/j.foodhyd.2017.12.033.

Dekkers, B. L., R. Hamoen, R. M. Boom, and A. J. van der Goot. 2018. Understanding fiber formation in a concentrated soy protein isolate - Pectin blend. *Journal of Food Engineering* 222:84–92. doi: 10.1016/j.jfoodeng.2017.11.014.

Dekkers, B. L., R. M. Boom, and A. J. van der Goot. 2018. Viscoelastic properties of soy protein isolate - pectin blends: Richer than those of a simple composite material. *Food Research International (Ottawa, Ont.)* 107:281–8. doi: 10.1016/j.foodres.2018.02.037.

Divoux, T., M. A. Fardin, S. Manneville, and S. Lerouge. 2016. Shear Banding of Complex Fluids. *Annual Review of Fluid Mechanics* 48 (1):81–103. doi: 10.1146/annurev-fluid-122414-034416.

Domenek, S., M. H. Morel, J. Bonicel, and S. Guilbert. 2002. Polymerization kinetics of wheat gluten upon thermosetting. A mechanistic model. *Journal of Agricultural and Food Chemistry* 50 (21):5947–54. doi: 10.1021/jf0256283.

Edwards, N. M., D. Peressini, J. E. Dexter, and S. J. Mulvaney. 2001. Viscoelastic properties of durum wheat and common wheat dough of different strengths. *Rheologica Acta* 40 (2):142–53. doi: 10.1007/s003970000147.

Einde, R. M., A. J. Goot, and R. M. Boom. 2003. Understanding molecular weight reduction of starch during heating-shearing processes. *Journal of Food Science* 68 (8):2396–404. doi: 10.1111/j.1365-2621.2003.tb07036.x.

Emin, M. A., and H. P. Schuchmann. 2013. Analysis of the dispersive mixing efficiency in a twin-screw extrusion processing of starch based matrix. *Journal of Food Engineering* 115 (1):132–43. doi: 10.1016/j.jfoodeng.2012.10.008.

Emin, M. A., and H. P. Schuchmann. 2017. A mechanistic approach to analyze extrusion processing of biopolymers by numerical, rheological, and optical methods. *Trends in Food Science & Technology* 60:88–95. doi: 10.1016/j.tifs.2016.10.003.

Emin, M. A., M. Quevedo, M. Wilhelm, and H. P. Karbstein. 2017. Analysis of the reaction behavior of highly concentrated plant proteins in extrusion-like conditions. *Innovative Food Science & Emerging Technologies* 44:15–20. doi: 10.1016/j.ifset.2017.09.013.

Evans, E. 2001. Probing the relation between force-lifetime-and chemistry in single molecular bonds. *Annual Review of Biophysics and Biomolecular Structure* 30:105–28. doi: 10.1146/annurev.biophys.30.1.105.

Fang, Y., B. Zhang, and Y. Wei. 2014. Effects of the specific mechanical energy on the physicochemical properties of texturized soy protein during high-moisture extrusion cooking. *Journal of Food Engineering* 121 (1):32–8. doi: 10.1016/j.jfoodeng.2013.08.002.

Fang, Y., B. Zhang, Y. Wei, and S. Li. 2013. Effects of specific mechanical energy on soy protein aggregation during extrusion process studied by size exclusion chromatography coupled with multi-angle laser light scattering. *Journal of Food Engineering* 115 (2):220–5. doi: 10.1016/j.jfoodeng.2012.10.017.

Geerts, M. E. J., B. L. Dekkers, A. van der Padt, and A. J. van der Goot. 2018. Aqueous fractionation processes of soy protein for fibrous structure formation. *Innovative Food Science & Emerging Technologies* 45:313–9. doi: 10.1016/j.ifset.2017.12.002.

Giezen, F. E., W. W. J. T. Jansen, and J. H. Willemsen. 2014. Method of making structured protein composites. https://www.freepatentsonline.com/20140127363.pdf.

Grabowska, K. J., S. Tekidou, R. M. Boom, and A. J. van der Goot. 2014. Shear structuring as a new method to make anisotropic structures from soy-gluten blends. *Food Research International (Ottawa, Ont.)* 64:743–51. doi: 10.1016/j.foodres.2014.08.010.

Grabowska, K. J., S. Zhu, B. L. Dekkers, N. C. A. De Ruijter, J. Gieteling, and A. J. Van Der Goot. 2016. Shear-induced structuring as a tool to make anisotropic materials using soy protein concentrate. *Journal of Food Engineering* 188:77–86. doi: 10.1016/j.jfoodeng.2016.05.010.

Grinberg, V. Y., and V. B. Tolstoguzov. 1997. Thermodynamic incompatibility of proteins and polysaccharides in solutions. *Food Hydrocolloids* 11 (2):145–58. doi: 10.1016/S0268-005X(97)80022-7.

Hansen, M. G., and S. Vedula. 1998. In-line fiber-optic near-infrared spectroscopy: Monitoring of rheological properties in an extrusion process. Part I. *Journal of Applied Polymer Science* 68 (6):859–72. doi: 10.1002/(sici)1097-4628(19980509)68:6 < 859::aid-app1 > 3.3.co;2-n.

Hatzikiriakos, S. G. 2012. Wall slip of molten polymers. *Progress in Polymer Science (Oxford)* 37 (4):624–43. doi: 10.1016/j.progpolymsci.2011.09.004.

Hine, P. J., S. W. Tsui, P. D. Coates, I. M. Ward, and R. A. Duckett. 1997. Measuring the development of fibre orientation during the melt extrusion of short glass fibre reinforced polypropylene. *Composites Part A: Applied Science and Manufacturing* 28 (11): 949–58. doi: 10.1016/S1359-835X(97)00070-5.

Hoek, A. C. 2010. Will novel protein foods beat meat? Consumer acceptance of meat substitutes - A multidisciplinary research approach. PhD thesis, Wageningen UR. http://library.wur.nl/WebQuery/clc/1926634.

Hörmann, T. R., J. Rehrl, O. Scheibelhofer, L. M. Schaden, A. Funke, C. Makert, and J. G. Khinast. 2019. Sensitivity of a continuous hot-melt extrusion and strand pelletization line to control actions and composition variation. *International Journal of Pharmaceutics* 566: 239–53. doi: 10.1016/j.ijpharm.2019.05.046.

Horvat, M., M. Azad Emin, B. Hochstein, N. Willenbacher, and H. P. Schuchmann. 2013. A multiple-step slit die rheometer for rheological characterization of extruded starch melts. *Journal of Food Engineering* 116 (2):398–403. doi: 10.1016/j.jfoodeng.2012.11.028.

Huang, X., Y. Lei, M. Wang, and G. Jin. 2018. In-line monitoring of component content of polypropylene/polystyrene blends during melt extrusion using Raman spectroscopy. *Journal of Raman Spectroscopy* 49 (3):513–9. doi: 10.1002/jrs.5309.

Hyun, K., M. Wilhelm, C. O. Klein, K. S. Cho, J. G. Nam, K. H. Ahn, S. J. Lee, R. H. Ewoldt, and G. H. McKinley. 2011. A review of nonlinear oscillatory shear tests: Analysis and application of large amplitude oscillatory shear (LAOS). *Progress in Polymer Science* 36 (12): 1697–753. doi: 10.1016/j.progpolymsci.2011.02.002.

Katsuta, K., and J. E. Kinsella. 1990. Effects of temperature on viscoelastic properties and activation energies of whey protein gels. *Journal of Food Science* 55 (5):1296–302. doi: 10.1111/j.1365-2621.1990.tb03920.x.

Klüver, E., and M. Meyer. 2015. Thermoplastic processing, rheology, and extrudate properties of wheat, soy, and pea proteins. *Polymer Engineering & Science* 55 (8):1912–9. doi: 10.1002/pen.

Krintiras, G. A., J. Gadea Diaz, A. J. Van Der Goot, A. I. Stankiewicz, and G. D. Stefanidis. 2016. On the use of the Couette Cell technology for large scale production of textured soy-based meat replacers. *Journal of Food Engineering* 169:205–13. doi: 10.1016/j.jfoodeng.2015.08.021.

Krintiras, G. A., J. Göbel, A. J. van der Goot, and G. D. Stefanidis. 2015. Production of structured soy-based meat analogues using simple shear and heat in a Couette Cell. *Journal of Food Engineering* 160:34–41. doi: 10.1016/j.jfoodeng.2015.02.015.

Kutzli, I., M. Gibis, S. K. Baier, and J. Weiss. 2019. Electrospinning of whey and soy protein mixed with maltodextrin – Influence of protein type and ratio on the production and morphology of fibers. *Food Hydrocolloids* 93:206–14. doi: 10.1016/j.foodhyd.2019.02.028.

Lagrain, B., B. G. Thewissen, K. Brijs, and J. A. Delcour. 2008. Mechanism of gliadin-glutenin cross-linking during hydrothermal treatment. *Food Chemistry* 107 (2):753–60. doi: 10.1016/j.foodchem.2007.08.082.

Lagrain, B., K. Brijs, and J. A. Delcour. 2008. Reaction kinetics of gliadin-glutenin cross-linking in model systems and in bread making. *Journal of Agricultural and Food Chemistry* 56 (22):10660–6. doi: 10.1021/jf801894r.

Lam, A. C. Y., A. Can Karaca, R. T. Tyler, and M. T. Nickerson. 2018. Pea protein isolates: Structure, extraction, and functionality. *Food Reviews International* 34 (2):126–47. doi: 10.1080/87559129.2016.1242135.

Leblanc, J. L. 2007. Nonlinear viscoelastic characterization of molten thermoplastic vulcanizates (TPV) through large amplitude harmonic experiments. *Rheologica Acta* 46 (8):1013–27. doi: 10.1007/s00397-007-0185-8.

Ledward, D. A., and R. F. Tester. 1994. Molecular transformations of proteinaceous foods during extrusion processing. *Trends in Food Science and Technology* 5 (4):117–20. doi: 10.1016/0924-2244(94)90200-3.

Leidy, R., and Q. C. Maria Ximena. 2019. Use of electrospinning technique to produce nanofibres for food industries: A perspective from regulations to characterisations. *Trends in Food Science & Technology* 85:92–106. doi: 10.1016/j.tifs.2019.01.006.

Lin, X. D., and W. L. Cheung. 1997. Effect of single screw extrusion through a round die on the morphology of POM/PP blends. *Journal of Materials Processing Technology* 63 (1–3):476–80. doi: 10.1016/S0924-0136(96)02668-4.

Liu, K. S., and F. H. Hsieh. 2007. Protein-protein interactions in high moisture-extruded meat analogs and heat-induced soy protein gels. *JAOCS. Journal of the American Oil Chemists' Society* 84 (8):741–8. doi: 10.1007/s11746-007-1095-8.

Liu, K. S., and F. H. Hsieh. 2008. Protein-protein interactions during high-moisture extrusion for fibrous meat analogues and comparison of protein solubility methods using different solvent systems. *Journal of Agricultural and Food Chemistry* 56 (8):2681–7. doi: 10.1021/jf073343q.

Manski, J. M., A. J. van der Goot, and R. M. Boom. 2007a. Advances in structure formation of anisotropic protein-rich foods through novel processing concepts. *Trends in Food Science & Technology* 18 (11):546–57. doi: 10.1016/j.tifs.2007.05.002.

Manski, J. M., A. J. van der Goot, and R. M. Boom. 2007b. Formation of fibrous materials from dense calcium caseinate dispersions. *Biomacromolecules* 8 (4):1271–9. doi: 10.1021/bm061008p.

Manski, J. M., E. E. J. van der Zalm, A. J. van der Goot, and R. M. Boom. 2008. Influence of process parameters on formation of fibrous materials from dense calcium caseinate dispersions and fat. *Food Hydrocolloids* 22 (4):587–600, 6. doi: 10.1016/j.foodhyd.2007.02.006.

Mendes, A. C., K. Stephansen, and I. S. Chronakis. 2017. Electrospinning of food proteins and polysaccharides. *Food Hydrocolloids* 68:53–68. doi: 10.1016/j.foodhyd.2016.10.022.

Metzner, A. B., and J. C. Reed. 1955. Flow of non-newtonian fluids-correlation of the laminar, transition, and turbulent-flow regions. *AIChE Journal* 1 (4):434–40. doi: 10.1002/aic.690010409.

Migler, K. B. 2001. String formation in sheared polymer blends: Coalescence, breakup, and finite size effects. *Physical Review Letters* 86 (6):1023–6. doi: 10.1103/PhysRevLett.86.1023.

Mitsoulis, E. 2010. Extrudate swell of Boger fluids. *Journal of Non-Newtonian Fluid Mechanics* 165 (13-14):812–24. doi: 10.1016/j.jnnfm.2010.04.011.

Mongruel, A., and M. Cartault. 2006. Nonlinear rheology of styrene-butadiene rubber filled with carbon-black or silica particles. *Journal of Rheology* 50 (2):115–35. doi: 10.1122/1.2167448.

Morel, M. H., A. Redl, and S. Guilbert. 2002. Mechanism of heat and shear mediated aggregation of wheat gluten protein upon mixing. *Biomacromolecules* 3 (3):488–97. doi: 10.1021/bm015639p.

Münstedt, H., and F. R. Schwarzl. 2014. *Deformation and flow of polymeric materials*. Berlin, Heidelberg: Springer. doi: 10.1007/978-3-642-55409-4.

Nagy, P. 2013. Kinetics and mechanisms of thiol-disulfide exchange covering direct substitution and thiol oxidation-mediated pathways. *Antioxidants & Redox Signaling* 18 (13):1623–41. doi: 10.1089/ars.2012.4973.

Ng, T. S. K., and G. H. McKinley. 2008. Power law gels at finite strains: The nonlinear rheology of gluten gels. *Journal of Rheology* 52 (2):417–49. doi: 10.1122/1.2828018.

Nieuwland, M., P. Geerdink, P. Brier, P. Van Den Eijnden, J. T. M. M. Henket, M. L. P. Langelaan, N. Stroeks, H. C. Van Deventer, and A. H. Martin. 2014. Food-grade electrospinning of proteins. *Innovative Food Science & Emerging Technologies* 20:269–75. doi: 10.1016/j.ifset.2014.07.006.

Noguchi, A. 1989. Chapter 11: Extrusion cooking of high-moisture protein foods. In *Extrusion cooking*, eds. C. Mercier, P. Linko, and J. M. Harper, 1st ed., 343–70. St. Paul, MN: American Association of Cereal Chemists.

O'Kane, F. E., R. P. Happe, J. M. Vereijken, H. Gruppen, and M. A. J. S. van Boekel. 2004. Heat-induced gelation of pea legumin: Comparison with soybean glycinin. *Journal of Agricultural and Food Chemistry* 52 (16):5071–8. doi: 10.1021/jf035215h.

Osen, R., S. Toelstede, P. Eisner, and U. Schweiggert-Weisz. 2015. Effect of high moisture extrusion cooking on protein-protein interactions of pea (Pisum sativum L.) protein isolates. *International Journal of Food Science & Technology* 50 (6):1390–6. doi: 10.1111/ijfs.12783.

Osen, R., S. Toelstede, F. Wild, P. Eisner, and U. Schweiggert-Weisz. 2014. High moisture extrusion cooking of pea protein isolates: Raw material characteristics, extruder responses, and texture properties. *Journal of Food Engineering* 127:67–74. doi: 10.1016/j.jfoodeng.2013.11.023.

Ozakisj, Y., A. Mizunolt, and K. Iriyamas. 1987. Inter- and intramolecular disulfide bond formation and related structural changes in the lens proteins. *Journal of Biologic* 262 (32):15545–51.

Palanisamy, M., S. Töpfl, R. G. Berger, and C. Hertel. 2019. Physico-chemical and nutritional properties of meat analogues based on Spirulina/lupin protein mixtures. *European Food Research and Technology* 245 (9):1889–98. doi: 10.1007/s00217-019-03298-w.

Pasquino, R., F. Snijkers, N. Grizzuti, and J. Vermant. 2010. The effect of particle size and migration on the formation of flow-induced structures in viscoelastic suspensions. *Rheologica Acta* 49 (10):993–1001. doi: 10.1007/s00397-010-0466-5.

Peighambardoust, S. H., A. J. Van Der Goot, R. J. Hamer, and R. M. Boom. 2004. A new method to study simple shear processing of wheat gluten-starch mixtures. *Cereal Chemistry Journal* 81 (6):714–21. doi: 10.1094/CCHEM.2004.81.6.714.

Peressini, D., S. H. Peighambardoust, R. J. Hamer, A. Sensidoni, and A. J. van der Goot. 2008. Effect of shear rate on microstructure and rheological properties of sheared wheat doughs. *Journal of Cereal Science* 48 (2):426–38. doi: 10.1016/j.jcs.2007.10.008.

Pietsch, V. L., H. P. Karbstein, and M. A. Emin. 2018. Kinetics of wheat gluten polymerization at extrusion-like conditions relevant for the production of meat analog products. *Food Hydrocolloids* 85:102–9. doi: 10.1016/j.foodhyd.2018.07.008.

Pietsch, V. L., J. M. Bühler, H. P. Karbstein, and M. A. Emin. 2019. High moisture extrusion of soy protein concentrate: Influence of thermomechanical treatment on protein-protein interactions and rheological properties. *Journal of Food Engineering* 251:11–8. doi: 10.1016/j.jfoodeng.2019.01.001.

Pietsch, V. L., M. A. Emin, and H. P. Schuchmann. 2017. Process conditions influencing wheat gluten polymerization during high moisture extrusion of meat analog products. *Journal of Food Engineering* 198:28–35. doi: 10.1016/j.jfoodeng.2016.10.027.

Pimentel, D., and M. Pimentel. 2003. Sustainability of meat-based and plant-based diets and the environment. *American Journal of Clinical Nutrition* 78(3 Suppl):660S–3S. doi: 10.1093/ajcn/78.3.660s.

Polyakov, V. I., V. Y. Grinberg, and V. B. Tolstoguzov. 1997. Thermodynamic incompatibility of proteins. *Food Hydrocolloids* 11 (2):171–80. doi: 10.1016/S0268-005X(97)80024-0.

Pommet, M., M. H. Morel, A. Redl, and S. Guilbert. 2004. Aggregation and degradation of plasticized wheat gluten during thermo-mechanical treatments, as monitored by rheological and biochemical changes. *Polymer* 45 (20):6853–60. doi: 10.1016/j.polymer.2004.07.076.

Ponrajan, A., T. Tonner, M. Okos, O. Campanella, and G. Narsimhan. 2020. Comparing inline extrusion viscosity for different operating conditions to offline capillary viscosity measurements. *Journal of Food Process Engineering* 43 (5):1–11. doi: 10.1111/jfpe.13199.

Puski, G., and A. H. Konwinski. 1976. Process of making a soy-based meat substitute.

Ralston, B. E., and T. A. Osswald. 2008. Viscosity of soy protein plastics determined by screw-driven capillary rheometry. *Journal of Polymers and the Environment* 16 (3):169–76. doi: 10.1007/s10924-008-0098-3.

Rehrah, D., M. Ahmedna, I. Goktepe, and J. Yu. 2009. Extrusion parameters and consumer acceptability of a peanut-based meat analogue. *International Journal of Food Science & Technology* 44 (10):2075–84. doi: 10.1111/j.1365-2621.2009.02035.x.

Ryle, A. P., and F. Sanger. 1955. Disulphide interchange reactions. *The Biochemical Journal* 60 (4):535–40. doi: 10.1042/bj0600535.

Samard, S., B. Y. Gu, and G. H. Ryu. 2019. Effects of extrusion types, screw speed and addition of wheat gluten on physicochemical characteristics and cooking stability of meat analogues. *Journal of the Science of Food and Agriculture* 99 (11):4922–31. doi: 10.1002/jsfa.9722.

Sandoval Murillo, J. L., R. Osen, S. Hiermaier, and G. Ganzenmüller. 2019. Towards understanding the mechanism of fibrous texture formation during high-moisture extrusion of meat substitutes. *Journal of Food Engineering* 242:8–20. doi: 10.1016/j.jfoodeng.2018.08.009.

Santos De Oliveira, I. S., A. Van Den Noort, J. T. Padding, W. K. Den Otter, and W. J. Briels. 2011. Alignment of particles in sheared viscoelastic fluids. *Journal of Chemical Physics* 135 (10):00219606. doi: 10.1063/1.3633701.

Schofield, J. D., R. C. Bottomley, M. F. Timms, and M. R. Booth. 1983. The effect of heat on wheat gluten and the involvement of sulphydryl-disulphide interchange reactions. *Journal of Cereal Science* 1 (4):241–53. doi: 10.1016/S0733-5210(83)80012-5.

Schreuders, F. K. G., B. L. Dekkers, I. Bodnár, P. Erni, R. M. Boom, and A. J. van der Goot. 2019. Comparing structuring potential of pea and soy protein with gluten for meat analogue preparation. *Journal of Food Engineering* 261:32–9. doi: 10.1016/j.jfoodeng.2019.04.022.

Schreuders, F. K. G., I. Bodnár, P. Erni, R. M. Boom, and A. J. van der Goot. 2020. Water redistribution determined by time domain NMR explains rheological properties of dense fibrous protein blends at high temperature. *Food Hydrocolloids* 101:105562. doi: 10.1016/j.foodhyd.2019.105562.

Schreuders, F. K. G., L. M. C. Sagis, I. Bodnár, P. Erni, R. M. Boom, and A. J. van der Goot. 2021. Small and large oscillatory shear properties of concentrated proteins. *Food Hydrocolloids* 110 (1):106172. doi: 10.1016/j.foodhyd.2020.106172.

Scirocco, R., J. Vermant, and J. Mewis. 2004. Effect of the viscoelasticity of the suspending fluid on structure formation in suspensions. *Journal of Non-Newtonian Fluid Mechanics* 117 (2–3):183–92. doi: 10.1016/j.jnnfm.2004.01.010.

Shewry, P. R., and A. S. Tatham. 1997. Disulphide bonds in wheat gluten proteins. *Journal of Cereal Science* 25 (3):207–27. doi: 10.1006/jcrs.1996.0100.

Shimada, K., and J. C. Cheftel. 1988. Determination of sulfhydryl groups and disulfide bonds in heat-induced gels of soy protein isolate. *Journal of Agricultural and Food Chemistry* 36 (1):147–53. doi: 10.1021/jf00079a038.

Son, Y. 2007. Determination of shear viscosity and shear rate from pressure drop and flow rate relationship in a rectangular channel. *Polymer* 48 (2):632–7. doi: 10.1016/j.polymer.2006.11.048.

Strecker, T. D., R. P. Cavalieri, R. L. Zollars, Y. Pomeranz. 1995. Polymerization and mechanical degradation kinetics of gluten and glutenin at extruder melt-section temperatures and shear rates. *Journal of Food Science* 60 (3):532–7. doi: 10.1111/j.1365-2621.1995.tb09820.x.

Thadavathi, Y. L. N., S. Wassén, and R. Kádár. 2019. In-line rheological and microstructural characterization of high moisture content protein vegetable mixtures in single screw extrusion. *Journal of Food Engineering* 245:112–23. doi: 10.1016/j.jfoodeng.2018.10.006.

Tolstoguzov, V. B. 1993. Thermoplastic extrusion—The mechanism of the formation of extrudate structure and properties. *Journal of the American Oil Chemists' Society* 70 (4):417–24. doi: 10.1007/BF02552717.

Tolstoguzov, V. B., A. I. Mzhel'sky, and V. Y. Gulov. 1974. Deformation of emulsion droplets in flow. *Colloid and Polymer Science* 252 (2):124–32. doi: 10.1007/BF01555536.

Udyarajan, C. T., D. S. Horne, and J. A. Lucey. 2007. Use of time-temperature superposition to study the rheological properties of cheese during heating and cooling. *International Journal of Food Science & Technology* 42 (6):686–98. doi: 10.1111/j.1365-2621.2006.01468.x.

van Dijk, E., A. Hoogeveen, and S. Abeln. 2015. The hydrophobic temperature dependence of amino acids directly calculated from protein structures. *PLoS Computational Biology* 11 (5):e1004277–17. doi: 10.1371/journal.pcbi.1004277.

Van Loon, S., J. Fransaer, C. Clasen, and J. Vermant. 2014. String formation in sheared suspensions in rheologically complex media: The essential role of shear thinning. *Journal of Rheology* 58 (1):237–01486055. doi: 10.1122/1.4853455.

Van Zuilichem, D. J. 1992. Extrusion cooking: Craft or science? PhD thesis, Wageningen University, 1–189. https://library.wur.nl/WebQuery/wurpubs/18873.

Velichko, E., B. Tian, T. Nikolaeva, J. Koning, J. van Duynhoven, and W. G. Bouwman. 2019. A versatile shear cell for investigation of structure of food materials under shear. *Colloids and Surfaces A: Physicochemical and Engineering Aspects* 566:21–8. doi: 10.1016/j.colsurfa.2018.12.046.

Vermant, J., and M. J. Solomon. 2005. Flow-induced structure in colloidal suspensions. https://iopscience.iop.org/article/10.1088/0953-8984/17/4/R02/meta.

Volkin, D. B., and A. M. Klibanov. 1987. Thermal destruction processes in proteins involving cystine residues. *Journal of Biological Chemistry* 262 (7):2945–50.

Wang, C. H., C. C. Huang, L. L. Lin, and W. Chen. 2016. The effect of disulfide bonds on protein folding, unfolding, and misfolding investigated by FT–Raman spectroscopy. *Journal of Raman Spectroscopy* 47 (8):940–7. doi: 10.1002/jrs.4935.

Yao, G., K. S. Liu, and F. Hsieh. 2004. A new method for characterizing fiber formation in meat analogs during high-moisture extrusion. *Journal of Food Science* 69 (7):303–7. doi: 10.1111/j.1365-2621.2004.tb13634.x.

Zhang, B., Y. Zhang, J. Dreisoerner, and Y. Wei. 2015. The effects of screw configuration on the screw fill degree and special mechanical energy in twin-screw extruder for high-moisture texturised defatted soybean meal. *Journal of Food Engineering* 157:77–83. doi: 10.1016/j.jfoodeng.2015.02.019.

Zhang, J., L. Liu, Y. Jiang, S. Faisal, Y. Xu, and Q. Wang. 2020. High-moisture extrusion of peanut protein-/carrageenan/sodium alginate/wheat starch mixtures: Effect of different exogenous polysaccharides on the process forming a fibrous structure. *Food Hydrocolloids* 2019:105311. doi: 10.1016/j.foodhyd.2019.105311.

Zhang, J., L. Liu, H. Liu, A. Yoon, S. S. H. Rizvi, and Q. Wang. 2019. Changes in conformation and quality of vegetable protein during texturization process by extrusion. *Critical Reviews in Food Science and Nutrition* 59 (20):3267–80. doi: 10.1080/10408398.2018.1487383.